Materials Science and Engineering B 263 (2021) 114857

Contents lists available at ScienceDirect

Materials Science & Engineering B

journal homepage: www.elsevier.com/locate/mseb

Ag^+ ion conduction in $AgI\text{-}Ag_2O\text{-}B_2O_3\text{-}P_2O_5$ glass electrolyte

V.A. Adhwaryu [a], D.K. Kanchan [b,*]

[a] Department of Science and Humanities, L. D. College OF Engineering, Ahmedabad 350 002, Gujarat, India
[b] Solid State Ionics and Glass Research Lab, Department of Physics, The M.S. University Of Baroda, Vadodara 390 002, Gujarat, India

ARTICLE INFO

Keywords:
Boro-Phosphate glass
Complex impedance spectroscopy (CIS)
Non bridging oxygen (NBO)
Activation energies (E_σ and E_τ)
Stretching parameter (β)
Frequency power exponent (n)
Decoupling index (R_τ)
Scaling behaviour of conductivity (σ') & electric modulus (M'')

ABSTRACT

The silver borophosphate glass system has been investigated using AgI as an additive halide. Electrochemical properties of the prepared glass electrolyte system $x.AgI:(100\text{-}x).[(30Ag_2O:(56B_2O_3\text{-}14P_2O_5))]$ has been prepared using conventional melt quenching technique. Structural characterization has been employed using XRD diffraction pattern to confirm the amorphous nature of the samples, FT-IR analysis is carried out to study the nature of the chemical bonding and different vibrational modes of structural units present in the composition. The glass transition (T_g) has been measured using TG/DTA technique. Electrical conductivity measurements have been carried out in the temperature range from 303 K to 373 K using complex impedance spectroscopy (CIS). The modulus formalisms along with stretching parameter (β) and decoupling index (R_τ) are calculated. The conductivity and modulus scaling of the prepared system using different models are studied. The present paper discusses the conduction mechanism and physical parameters of conductivity.

1. Introduction

Fast ion conducting (FIC) glasses are the materials that exhibit electrical conductivity by means of the motion of ions (cations/anions) in an amorphous phase. Generally, FIC glasses exhibit much higher ionic conductivity and isotropic property due to lack of long-range order compare to their crystalline counterparts. The developments of ion-conducting glassy electrolytes have been gradually increased due to wide range composition which gives better control over properties. Fast ion (silver) conducting glasses was first reported by Kunze [1] and it is considered as one of the most promising candidate for application in various electrochemical devices such as gas sensors, fuel cells, super-capacitors, solar cells. Apart from this, it has also been widely applied for battery materials as a solid-state electrolyte in a solid-state battery [2–6] where physical properties can be tuned by varying chemical composition.

The key constituents in an ion conducting glass are the glass former, glass modifier and additive salt as well. The glass former provides a frozen skeleton, whereas the metal oxide modifies a network linkage and produces Non-Bridging Oxygen (NBO). It is found that the simultaneous presence of two glass formers [7–10] enhance the ion conducting properties. The phosphate glasses can be used as fast ion conductors, optical waveguides and fibres, etc. However, the applications of these glasses are often limited due to their low chemical durability [11]. It is observed that such chemical durability can be enhanced either by replacing of P_2O_5 by B_2O_3 or mixing both which transforms the structure of borophosphate glasses from linear-chain structure of metaphosphate glass into three-dimensional structure of borophosphate glass [12]. The additive salt like MX (metal halide) provides cationic conduction in a tailored glass structure. Amongst all the metal halides AgI is the model material in which Ag^+ ions surrounded by I^- are responsible for high conductivity especially when it is in α–AgI phase [13,14]. Suresh Kumar et al. [14], have reported the ionic conductivity of the order of $10^{-6}\ \Omega^{-1}\ cm^{-1}$ at 293 K for silver oxysalt such as $Ag_2O\text{-}V_2O_5$ doped with CuI. It is also a well established fact that AgI has a characteristic disordered structure in alpha phase, shows an abrupt increase in conductivity more than three orders of magnitude during solid to solid phase transformation at around 420 K temperature. It is interesting to note that the glasses which are suitable to house α–AgI phase at room temperature being by virtue of low activation barrier for ion migration results into high ionic conductivity. According to hard and soft (Lewis) acids and bases (HSAB) theory, AgI compound composed of soft Lewis acid (Ag^+) and soft base (I^-) in which the iodide ion has much larger ionic radius than the silver cation. Between two iodide ionic spheres, relatively larger chinks have been formed since the silver ion is somewhat soft due to large polarizibility [15]. In AgI doped ionic glass, Ag^+ possess shallow potential well and is loosely bound with iodide which, in turn, softens the host glassy matrix. This high decoupling of ions

* Corresponding author.
E-mail addresses: vaishali.adhwaryu@ldce.ac.in (V.A. Adhwaryu), dkkanchan.ssi@gmail.com (D.K. Kanchan).

https://doi.org/10.1016/j.mseb.2020.114857
Received 30 April 2020; Received in revised form 11 September 2020; Accepted 1 October 2020
Available online 2 November 2020

Table 1
Various amounts of AgI in silver borophosphate glass electrolyte system.

Sample code	Glass former (wt.%) (B_2O_3-P_2O_5)	Glass modifier (wt.%) (Ag_2O)	Additive (wt.%) (AgI)
ABP0	70	30	0
ABP1	69.3	29.7	1
ABP3	67.9	29.1	3
ABP5	66.5	28.5	5
ABP7	65.1	27.9	7

supports the movement of ions. According to Deshpande et al.; [16], dopant salts such as LiCl to the lithium borate and lithium borosilicate glasses, the decoupled charge carriers (Li^+) go on successive jumps from one NBO to the another to give rise to conduction. Consequently, silver ions from AgI can be decoupled which can easily migrate and diffuse through the openings formed by anionic spheres in the glassy amorphous structure, allowing fast cationic conduction even with the lower concentration of AgI [1,13,17]. Various Research groups have reported conduction mechanism in different glass systems wherein AgI as an additive salt is used. Minami et al.;[18], studied $AgX-Ag_2O-B_2O_3$ glass system, discussed the temperature and composition dependent behaviour of ionic conductivity, and reported the room temperature ionic conductivity of the order of $10^{-2}\ \Omega^{-1}\ cm^{-1}$. While the maximum conductivity at 303 K for silver borophosphate glass is about $10^{-5}\ \Omega^{-1}\ cm^{-1}$ [19]. P. Sharma et al; have reported the increase in ionic conductivity with the concentration of AgI salt in $AgI-Ag_2O-V_2O_5-TeO_2$ glass system [20]. Principally, the ionic conductivity in glassy electrolytes is governed by the number of NBOs' (of the host matrix) and the number of mobile charge species.

Therefore, it is interesting and novelty to study systematic variations of AgI salt in an otherwise very rigid boro-phosphate glassy system. In the present system, we have varied the ionic salt AgI in x.AgI:[(100-x).($30Ag_2O$:$70(B_2O_3$-$P_2O_5)$)] to understand how ionic conduction occurs in a rigid silver boro-phosphate glass system.

2. Experimental

The basic materials such as Boric Acid (H_3BO_3) from BDH, India, Ammonium dihydrogen phosphate (ADP-$NH_4H_2PO_4$) from HiMedia Laboratory, Silver Oxide (Ag_2O) from Qualigens Fine Chemicals, and Silver Iodide (AgI) from National Chemicals were procured. The ionic glass samples were prepared by taking appropriate amount of the chemicals, thoroughly mixed them in agate mortar pestle and then pre heated at about 450°C for 2 h to remove the gases from the chemicals. Subsequently, the mixture was melted at around 800°C for 6 h and then quenched between two pre cooled copper blocks [20]. The glass samples were transparent to pale yellow and then to orange colour depending upon the concentration of AgI in a glass composition. These samples were kept in a furnace for an hour at 150°C temperature for annealing to remove thermal stress [20,21]. The solid glassy electrolyte samples with variation in AgI concentration are listed in the Table 1.

3. Characterization

We have measured the density using Archimedes principle, X-ray diffraction (XRD) pattern to confirm amorphous nature of the

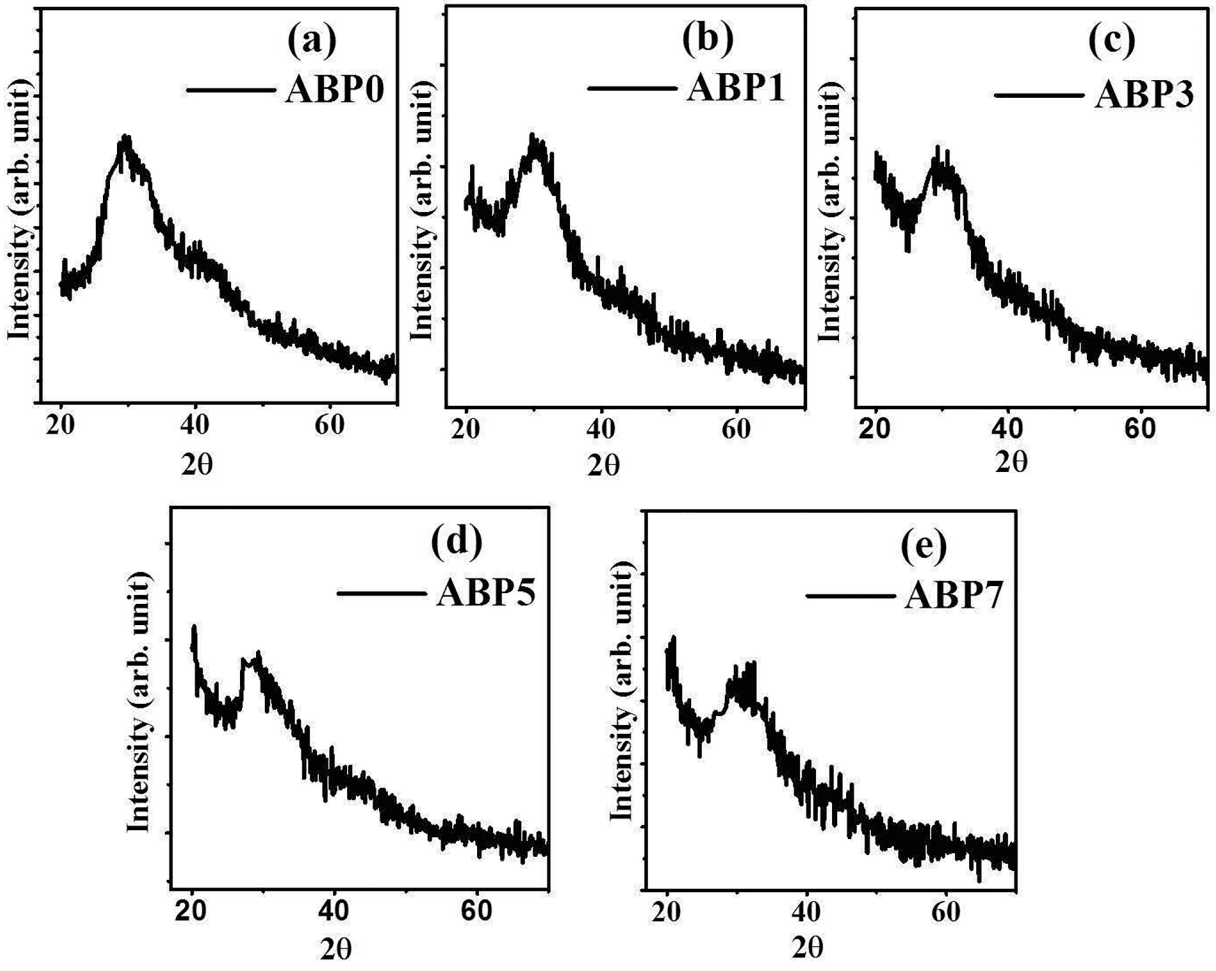

Fig. 1. X-ray diffraction pattern of different glassy electrolyte samples from ABP0 to ABP7.

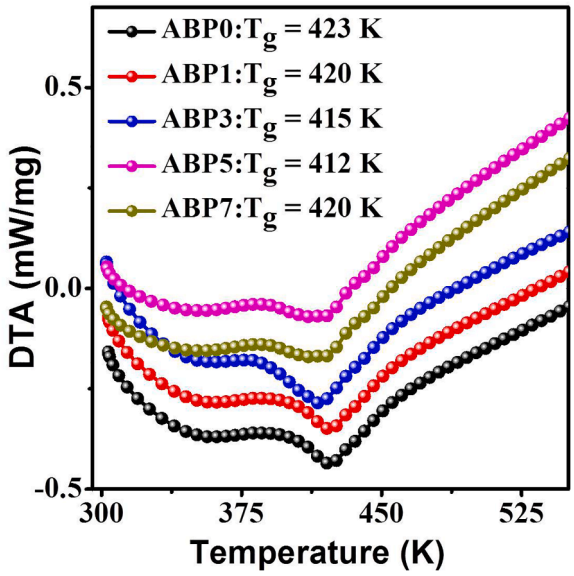

Fig. 2. DTA thermograms for glass transition temperature (T_g) of all glassy electrolytes.

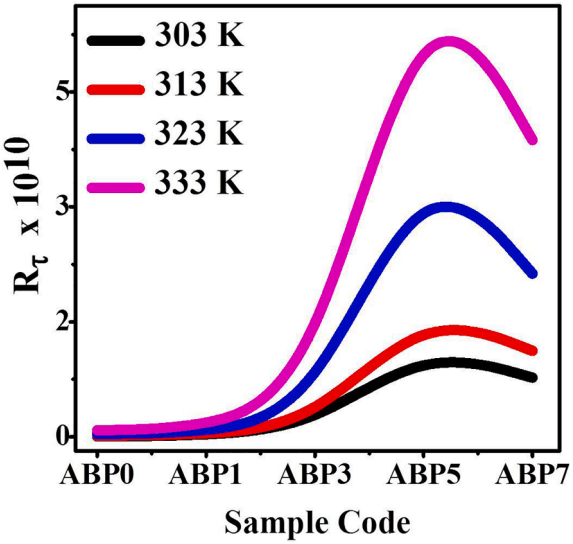

Fig. 3. Variation of decoupling index (R_τ) with composition at various temperature.

electrolyte. Fourier Transform Infrared spectroscopy (FT-IR) for any change in molecular bonds, thermal analysis for glass transition temperature (T_g) and complex impedance spectroscopy (CIS) for the conductivity and related parameters to understand the silver ion motion hence conduction in silver boro-phosphate glass system.

3.1. Density measurement

The density of the glassy electrolytes was determined by Archimedes principle. Acetone (being volatile in nature) was used as a reference liquid, which has the density of 0.791 g/cc. From the density measurements, molar volume, cation concentration and inter atomic distance have been measured [9].

3.2. X-ray diffraction

X-ray diffraction, a powerful non-destructive technique, provides the information about crystallinity and the structural changes in a sample. The structure of prepared glassy electrolyte samples is examined by means of X-ray diffraction analysis. XRD patterns deduced with the help of "D8-Discovery high-temp Bruker" machine using Cu-Kα X-rays with $\lambda = 0.154056$ nm operating over the 2θ range from 20°-70° in the step of 0.05°.

3.3. FTIR spectroscopy

FT-IR spectra were taken on pellets of KBr and glass samples using FTIR-4100 JASCO model over the range of wave number of 400 cm^{-1} to 1700 cm^{-1} with the scanning rate of 2 mm/sec.

3.4. Thermogravimetry-Differential Thermal Analysis (TG-DTA)

Thermal analysis in terms of glass transition temperature (T_g) of all the samples was obtained using TG-DTA with the model NETZSCH STA 449F3, by the heating rate of 2.3 (Kelvin per min) over the temperature range of 303 K to 1273 K.

3.5. Complex Impedance Spectroscopy (CIS)

The ionic conductivity of the glassy electrolyte is measured by a high precision Solartron-1260A impedance analyser in the frequency range 1 Hz-32 MHz at various temperatures between 303 K to 373 K. To measure impedance at different frequencies, silver painted glassy samples of certain shape and width were sandwiched between two blocking (silver) electrodes placed in a sample holder. This assembly was then kept in a furnace for measuring the impedance as a function of temperature and frequency. The bulk conductivity [22,23] of each glassy sample was calculated using the Equation (1).

$$\sigma_b = \frac{t}{R_b.A} \tag{1}$$

where t is the thickness of the samples, R_b is the bulk resistance, A is the area of the electrolyte - electrode contact.

4. Results and discussion

4.1. Structural Analysis

The XRD patterns of all glassy electrolytes shown in Fig. 1 depict a broad hump at about at $2\theta \sim 29^\circ$ and no crystalline peak anywhere in the spectra suggesting a complete amorphous nature of prepared electrolyte samples. The addition of AgI does not show any new peak or phase in any sample but a slight shift of peak between $2\theta \sim 27^\circ - 28^\circ$ in ABP5. No sharp peak in any of the spectra confirms a complete dissolution of AgI in an amorphous phase. Thermal analysis is shown in Fig. 2, indicates that the values of T_g decrease from 423 K to 412 K when an amount of AgI varies from 0 to 5 wt% respectively. It also upholds the result described by Angell that the gradual decreases in T_g with the addition of AgI due to rupturing of glass structure, cations to modify the structure as well [24]. After that T_g increases to 420 K for ABP7 sample. The shift of the T_g in the present system towards low temperature side can be attributed to decrease of rigidity of the glass structure and increase in non-bridging oxygen in the structure. While, at 7 wt% of AgI, the rigidity of the structure increases may be due to increase in glass transition temperature. J. Shelby also showed that the structure is modified by not only modifier but additive AgI also participates in modifying the glass [25]. This produces more number of non-bridging oxygen (NBOs) into the structure and higher number of NBOs, in turn, lowers the viscosity (softening) of the glass. The decoupling index profile as a function of temperature and glass composition is shown in Fig. 3. The decoupling index is an indicative of number of decoupled ions from the parent glassy matrix. In the present study, the decoupling index increases up to 5 wt% of AgI addition in a glass composition and

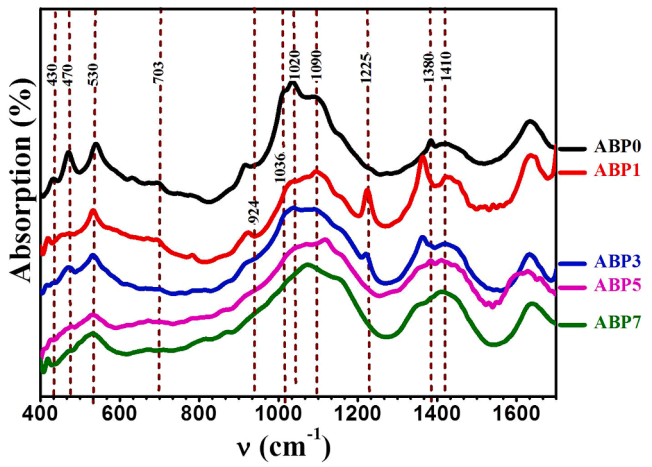

Fig. 4. FTIR absorption spectra of all glass samples between 400 cm^{-1} to 1700 cm^{-1} wave number.

Table 2
Summary of FTIR Absorption features and their assignments for various functional groups present in the present glass system.

Wavenumber (cm^{-1})	Mode Of Vibration	Assignment Of IR Band	Reference
~430–470	Bending (δ_s)	O-P-O bonds (of PO_4^{3-} group) and O-B-O bond	[26]
530	Bending (δ_s)	O = P-O bonds due to deformation mode of PO^-	[26,27]
~670–730	Bending (δ_s) Symmetric (ν_s)	B-O-B linkage in various borate unit P-O-P bridge	[28-31]
~924	Symmetric stretching (ν_s)	P-O-P chain of PO_4^{3-} group	[26,27,31]
~1020–1030	Asymmetric stretching (ν_{as}) Symmetric stretching (ν_s)	B-O bond of BO_4^{3-} tetrahedron unit PO_3 unit	[18,27,32–34]
~1090–1120	Asymmetric stretching (ν_{as})	$P-O^-$ group of orthophosphate (PO_4^{3-})	[27,33,34]
~1130–1160	Asymmetric stretching (ν_{as})	BO_3^- of penta borate unit	[28,30]
~1225	Asymmetric stretching (ν_{as})	Metaphosphate $(PO_2)^-$ group	[27,31]
~1330–1360	Symmetric stretching (ν_s)	pyro and ortho borate groups in BO_3 unit	[18,30]
~1385–1339	Asymmetric stretching (ν_{as})	P = O in NBO atom of phosphate chain	[26]
~1410–1420	Asymmetric stretching (ν_{as})	Borate triangle unit (BO^-).	[30]
~1450–1460	Asymmetric stretching (ν_{as})	B-O stretching of triangle BO_3^- and BO_2^- unit	[30]
~1620–1640	————	P-O-H bond	[26,27]
~1700	Asymmetric stretching (ν_{as})	B-O-B in BO_3 triangles	[32]

then after decreases beyond this [18].

4.2. Fourier Transform Infrared spectroscopy (FTIR) study

FTIR spectrum has been analysed to study any change observed in vibrational bond lengths of molecular structure which oscillates only at certain quantized frequency. The spectra reveal the molecular structure and detect the presence of functional groups in it. In the present study, the FT-IR absorption spectra is recorded for the wave number from 400 cm^{-1}-1700 cm^{-1} as shown in Fig. 4. The wave number of the peaks, their corresponding vibrational modes and respective IR band assignments are listed in Table 2.

The intensity of peaks observed at 430 cm^{-1} and 470 cm^{-1} decreases with addition of AgI in the system. P-O-P bending peak at 530 cm^{-1}, does not show any significant change with addition of AgI, while, B-O-B bending peak [29] gradually shifts from 703 cm^{-1} to 670 cm^{-1} [32]. With addition of AgI which suggests increase the bending motion of B-O-B bond. The peak intensity of the wavenumber in the range 1080 cm^{-1}-1090 cm^{-1} corresponds to $P-O^-$ symmetric stretching [34,35] which increases till 5 wt% but for ABP7 sample, the peak intensity reduces. An increase in peak intensity suggests increase in number of PO^- molecules and a new absorption peak at 1225 cm^{-1} emerges for AgI up to 3 wt% which corresponds to asymmetric vibration of PO_2 group [34]. The IR band corresponding to asymmetric vibration of P = O [26] in phosphate chain is observed at around 1385 cm^{-1} for ABP0 sample which shifts gradually towards lower frequency up to 1349 cm^{-1} for ABP7. Intensity of this peak also decreases with AgI concentration. Ag^+ ions from AgI, when added in the system interstitially, starts influencing this P = O bond and the bond length starts increasing. It means the P = O bond gets stretched and a shift in IR frequency towards lower wave number is expected. The absorption band at 1410 cm^{-1} [30] which belongs to asymmetric stretching of trigonal borate unit, remains unaffected in all the glass samples. The vibration of P-O-H bond [26,27] appears at around 1638 cm^{-1}, for ABP0 which also shifts gradually with the addition of AgI in the glass structure. This peak is attributed to the water content absorbed while preparing KBr pellets for IR measurements.

The broadened band in the range 800 cm^{-1}-1200 cm^{-1} and 1300 cm^{-1}-1500 cm^{-1} of IR spectrum have been deconvoluted to understand the peaks or polyhedra of B_2O_3 and P_2O_5 which combined to give the broadened peak in IR spectra.

Deconvolution spectra between the wavenumber range 800 cm^{-1}-1200 cm^{-1} for all the glass samples are shown in Fig. 5. The peak at 924 cm^{-1} corresponding to asymmetric vibration of PO_4^{3-} [26,27,31] remains nearly constant with increasing intensity with AgI and is not observed at 7 wt% of AgI sample. Asymmetric vibration of BO_4 [32] and PO_4 [34] units at around 1030 cm^{-1} and at ≈1098 cm^{-1} [33] respectively are observed whereas peak at ≈1143 cm^{-1} [28,30] belonging to BO_3^- also show increasing intensity with the addition of silver salt.

IR spectrum, deconvoluted for the wavenumber ranging from 1300 cm^{-1}–1500 cm^{-1} shown in Fig. 6, reveal four absorption bands. Peak at around 1369 cm^{-1} [18] belongs to symmetric stretching of pyro and ortho borate group of BO_3 molecule which suddenly shifts to 1339 cm^{-1} at 7 wt% of AgI. The asymmetric vibration of borate triangle unit shows absorption peak at ≈1411 cm^{-1} [30]. The intensity of this peak enhances with the addition of AgI. Asymmetric stretching bands observed at approximately 1460 cm^{-1} [30] corresponding to BO_3^- and BO_2^- units respectively do not change. Hence, it can be concluded from FTIR spectra that an increase in B-O bond length of BO_4 and BO_3^- units, formation of asymmetric PO_4^{3-} molecules and P-O-B linkages units are formed with the addition of AgI in the structure.

4.3. Conductivity analysis

Complex impedance spectroscopy (CIS) of electro material has been analysed using impedance formalism technique. The conductivity study is done over the temperature range from 303 K to 373 K and the frequency ranges from 1 Hz to 32 MHz. The real ($Z^{'}$) and imaginary ($Z^{''}$) of the impedance for all the compositions at 318 K temperature are shown in the form of Nyquist plot in Fig. 7(a). The depressed semi-circle of the plot suggests that the sample consists of parallel combination of resistive (R), capacitive (C) and Warburg (W) components distributed inhomogeneously. The observed plot of silver borophosphate glass electrolyte containing 5 wt% AgI is fitted with the equivalent circuit as shown in Fig. 7(b). The semicircle in high frequency region in $Z^{'}$ Vs. $Z^{''}$ plot corresponds to the kinetic controlled charge transfer mechanism, whereas,

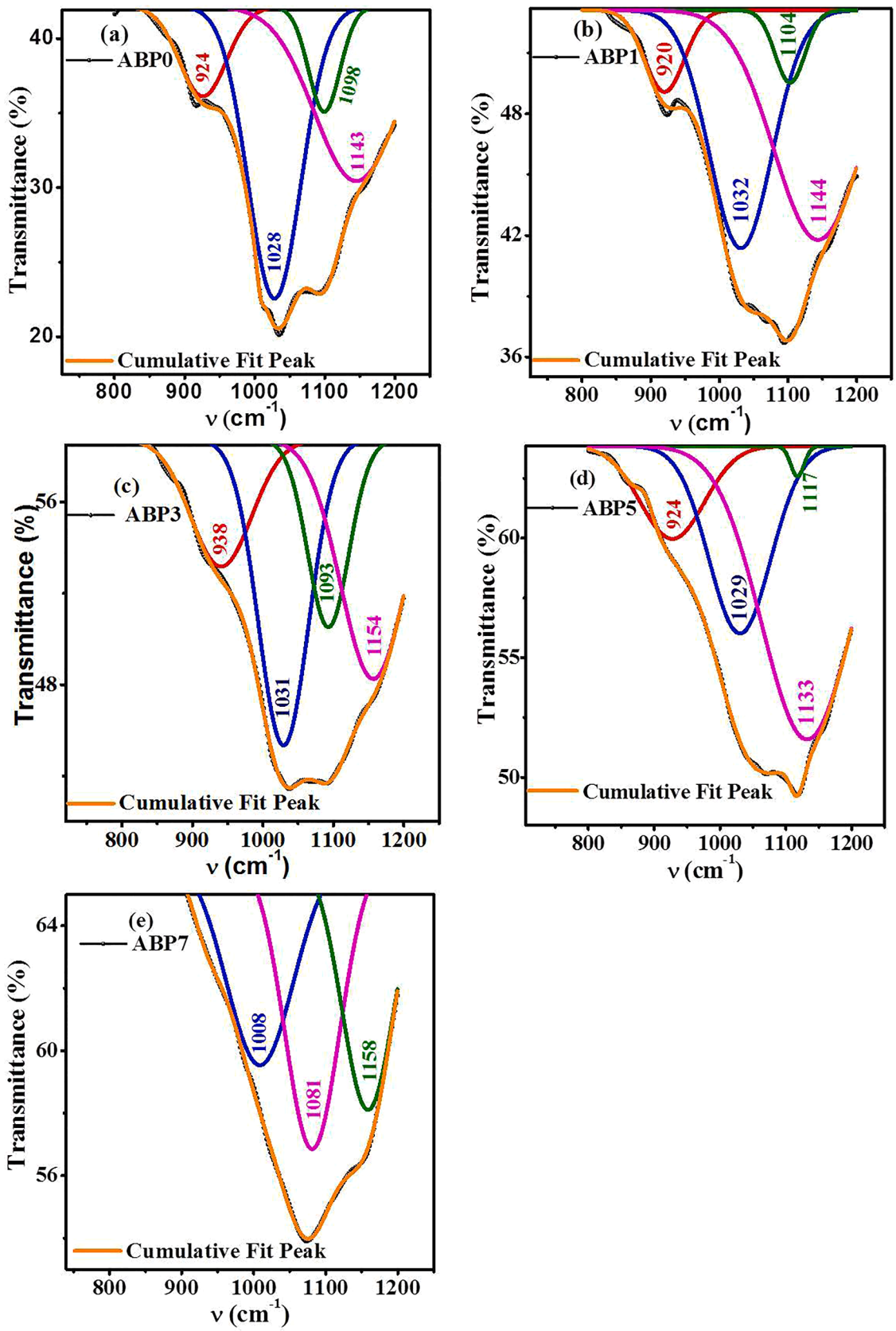

Fig. 5. (a-e) Deconvoluted FTIR spectra in the wavenumber range from 800 cm^{-1} to 1200 cm^{-1} for ABP0 to ABP7 samples.

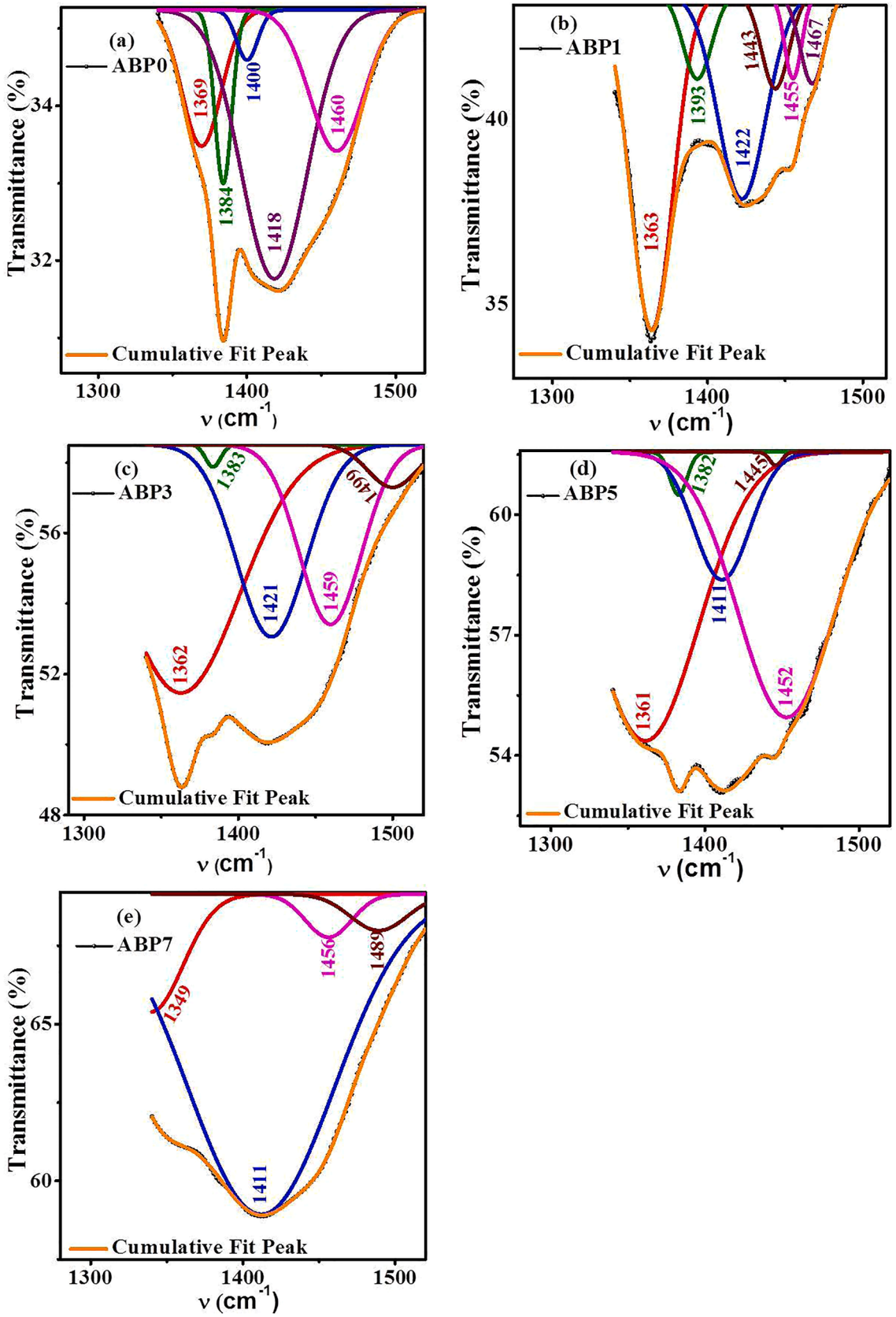

Fig. 6. (a-e) Deconvoluted FTIR spectra in the wavenumber range from 1300 cm^{-1} to 1500 cm^{-1} for ABP0 to ABP7 samples.

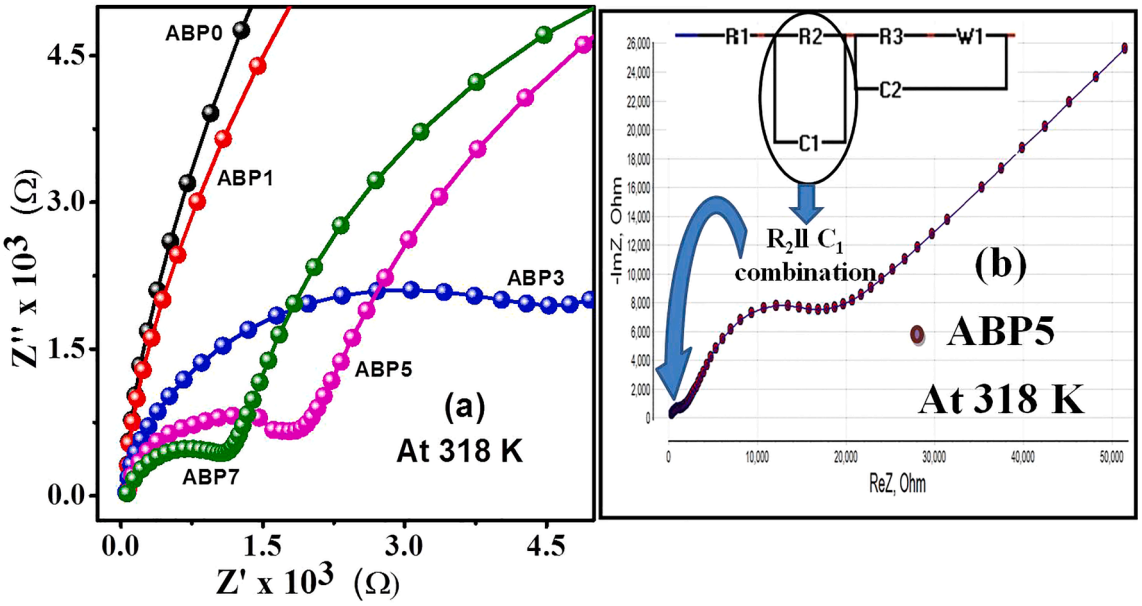

Fig. 7. (a) Nyquist plot of all glassy electrolytes at 318 K temperature, (b) Nyquist plot fitting and its equivalent circuit for ABP5 sample at room temperature.

Table 3
Activation energy (E_σ), dc conductivity (σ_{dc}), decoupling index (R_τ), carrier concentration (K'), hopping frequency (ω_p), relaxation time (τ_c), stretching component (β) of the AgI doped silver borophosphate glass system.

Sample Code	Activation energy E_σ (eV)	Calculated at 303 K					
		Conductivity σ_{dc} (S cm^{-1})	Decoupling index Rτ	Hopping frequency ω_p (Hz)	Carrier concentration K' (Ω^{-1} cm^{-1} Hz^{-1} K)	Relaxation time τ_c (second)	Stretching component β
ABP0	0.84	2.42×10^{-7}	4.84×10^{7}	4.75×10^{5}	1.09×10^{-11}	2.11×10^{-6}	0.452
ABP1	0.69	5.86×10^{-7}	1.17×10^{8}	6.01×10^{5}	3.28×10^{-11}	1.66×10^{-6}	0.453
ABP3	0.56	7.19×10^{-6}	1.44×10^{9}	5.95×10^{6}	1.39×10^{-10}	1.68×10^{-7}	0.564
ABP5	0.49	6.24×10^{-5}	1.25×10^{10}	3.06×10^{7}	1.15×10^{-9}	3.27×10^{-8}	0.728
ABP7	0.52	4.12×10^{-5}	8.24×10^{9}	1.32×10^{7}	6.17×10^{-10}	7.56×10^{-8}	0.796

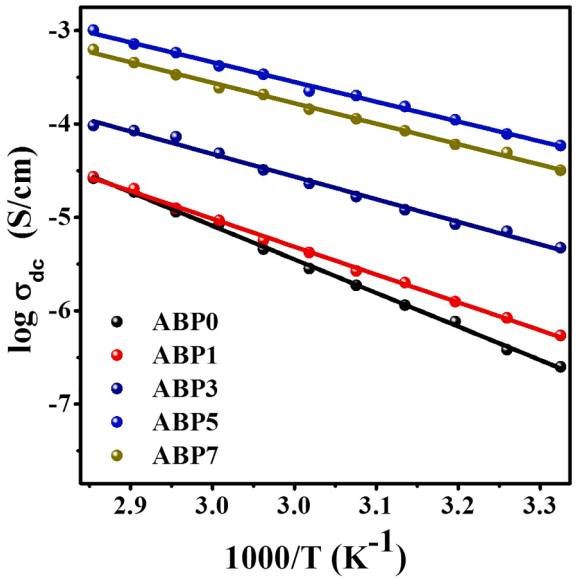

Fig. 8. Log of dc conductivity vs. 1000/T plot of all glass samples.

the low frequency region spike is because of the double layer formation (C_{dl}) which is a result of accumulation of charges at the electrolyte–electrode interface [2]. It is clear from Fig. 7(a) that the intercept of the plots on the real axis (Z') decreases as the concentration of AgI increases. From the Nyquist plot, bulk resistance (R_b), and hence, the conductivity of glassy electrolyte material is calculated and listed in Table 3. It is seen from the Table 3 that the bulk conductivity of AgI-Ag_2O-B_2O_3-P_2O_5 glassy electrolyte system increases upon addition of AgI till 5 wt%. and decreases for 7 wt% of AgI in the glass. The conductivity of 8.35×10^{-5} (Ω cm) $^{-1}$ has been observed for lithium phosphate system [23]. Two ion transport models namely (i) Arrhenius behaviour and (ii) Nonlinear behaviour are generally being used for temperature dependent ionic conductivity in disordered systems [36]. Ion hopping mechanism for conduction shows Arrhenius behaviour as given in Equation 2.

$$\sigma_{dc} = \sigma_0 \ exp(-E_\sigma/K_B T) \quad (2)$$

The plot of log of σ_{dc} vs. 1000/T is typically linear depicted in Fig. 8. It is noted that the activation energy E_σ which was calculated using the slope of the plots [36] given in Fig. 8. For ABP0, the activation energy is observed to be 0.84 eV and with the addition of AgI, it decreases to 0.49 eV for ABP5, however, it increases to 0.52 eV for 7 wt% AgI sample as given in Table 3. The variation of σ_{dc} at 323 K and activation energy (E_σ) for AgI-Ag_2O-B_2O_3-P_2O_5 glassy electrolyte system are shown in Fig. 9 (a and b) which show increase in conductivity while activation energy follows the reverse behaviour as expected [36] till 5 wt% of AgI. Silver (Ag) and iodine both are known as soft acid and base and are easily dissociated into Ag^+ and I^- ions in AgI. Silver ions from AgI act as a modifier and encourage the formation of apparently more non-bridging oxygen groups in the structural network till 5 wt% of AgI as is evident from FTIR study.

The cause of reduction in activation energy and increase in conductivity may be understood on the basis of the Anderson-Stuart (A-S)

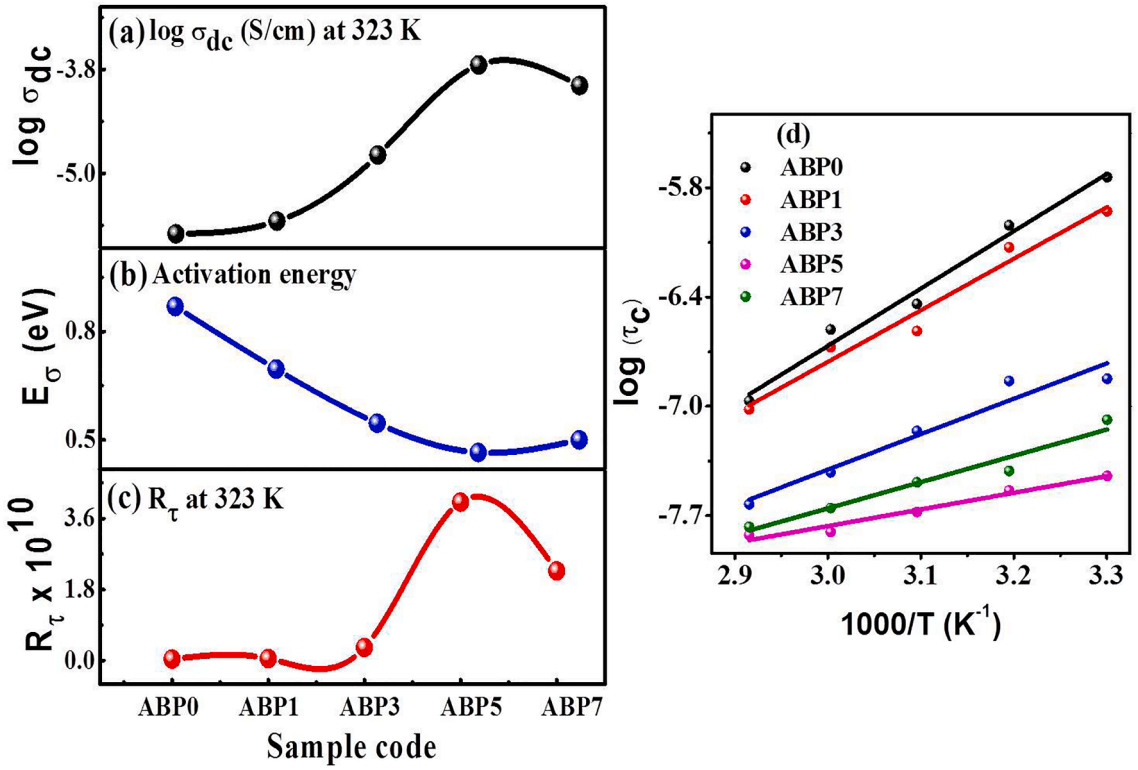

Fig. 9. (a-d): (a) Variation of σ_{dc}, (b) Activation energy (E_σ), and (c) Decoupling index (R_τ) with AgI concentration (d) Plot of relaxation time (τ_c) vs. reciprocal of temperature for all glass compositions.

model of ion conduction in glasses [37–39]. According to the Anderson-Stuart model of ion conduction, the total activation energy $\mathbf{E}_\sigma$ for a successful hop of an ion may be considered to be a sum of two fractions: $\mathbf{E}_\sigma = \mathbf{E_b} + \mathbf{E_S}$. Here, $\mathbf{E_b}$ is the binding energy which is the mean energy that a cation needs to leave its site and the other one is $\mathbf{E_S}$, the elastic strain energy. The elastic strain energy is the mean kinetic energy that a cation needs to open a 'doorway' in the structure of the glass to pass through, which involves the energy to overcome the electrostatic forces between Ag^+ ions, the neighbouring oxygen and iodide ions. It is reported by Ghosh et.al.; [34], that hopping of positive alkali ions occurs between different types of borate and phosphate sites present in the borophosphate glass skeleton. Hence, amongst all the preferable anionic sites such as PO_4^3, PO^{-2}, BO_4^3 which are being formed with the addition of AgI in the glass structure, if the silver ions are trapped in a shallow potential well (requires less activation energy) and may increase the pathways for the migration of mobile cationic species and enhances the conductivity up to 5 wt% of AgI. Beyond this, Ag ions start changing their local coordination from exclusively oxygen to entirely I^-

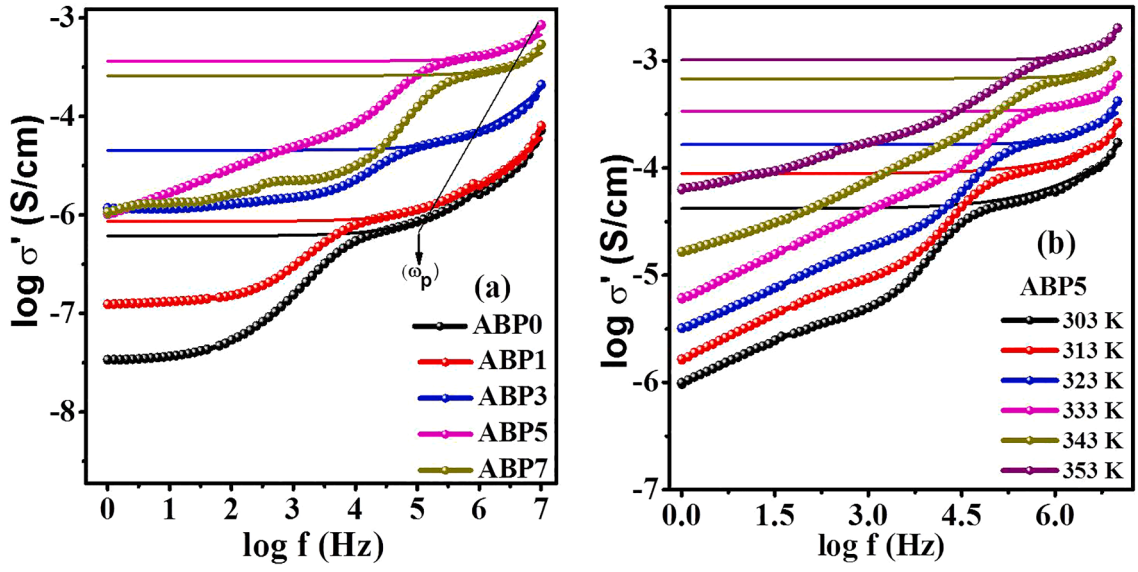

Fig. 10. (a) Variation of ac conductivity as a function of log frequency of all glass samples with at 323 K, (b) Variation of log ac conductivity of ABP5 as a function of log frequency at different temperatures.

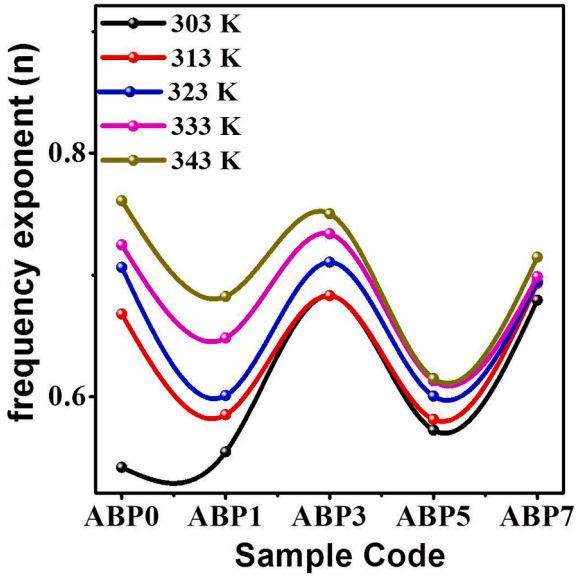

Fig. 11. Frequency exponent (n) as a function of glass compositions at various temperatures.

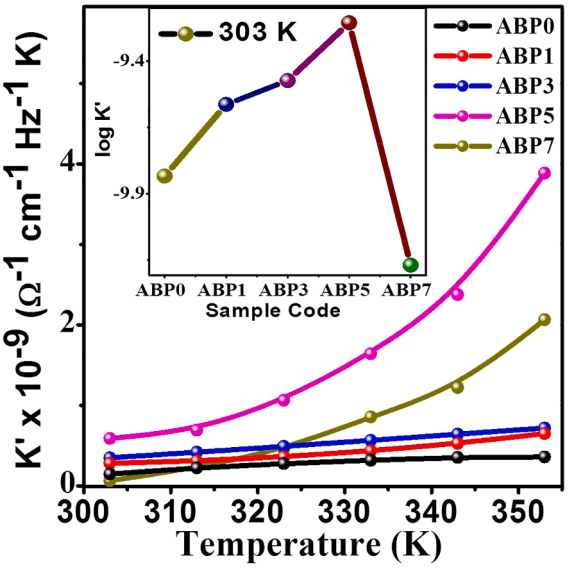

Fig. 12. Variation of mobile ion concentration ($K^{'}$) as function of temperature for ABP glass compositions.

environment to induce a reduction in the conductivity or an increase in activation energy, $\mathbf{E}_{\sigma}$.

The variation in conductivity with composition is also confirmed by the decoupling index R_{τ} values plotted in Fig. 9(c). Decoupling index, R_{τ}, in an ionically conducting glass system, is a measure of how strongly the mobile ions are decoupled from the glass matrix [24]. It is defined as the ratio of the average structural relaxation time τ_s at T_g to the average conductivity relaxation time τ_c at T_g. Generally, $\tau_s = 200$ s at T_g [40], while the τ_c at T_g values were determined by extrapolating the $\log\tau_c \rightarrow 1000/T$ graph to T_g shown in Fig. 9(d). One may also note from Table 3 that with increasing AgI content, R_{τ} values steadily increase till 5 wt% amount of AgI in the glass composition. This rise in decoupling index suggests that the viscosity of the glass structure network must be reducing which favours the migration of Ag^{+} ions. Hence, because of the rise in decoupling index with AgI, the motion of Ag^{+} ions are becoming easier, because they get more and more decoupled or free from the glass matrix for transport.

4.4. Frequency dependent conductivity

The Fig. 10(a) shows the variation of ac conductivity (σ_{ac}) as a function of frequency for different amount of AgI in ABP glass compositions at 323 K while Fig. 10(b) shows the variation of ac conductivity (σ_{ac}) as a function of frequency at different temperatures for ABP5. There are generally three crossover regions present; one appearing in the lower frequency region, occurs due to polarization effects at the electrodes, while the another in the mid frequency region shows frequency independent plateau and the last is dispersion region in the high frequency region where conductivity increases rapidly with frequency. The plateau region, where $\sigma(f)$ is zero, is extrapolated to find out the σ_{dc} value [22,23]. The frequency dependent conductivity data were analysed using Jonscher's universal power law using Equation (3),

$$\sigma'(\omega) = \sigma_{ac} = (\sigma_{dc} + A\omega^{n}) \tag{3}$$

where A is a constant, ω is the radial frequency and n is the frequency dependent exponent factor. The frequency response of conductivity in glasses may be entirely due to the translational and localized hopping of ions [41]. The translational hopping gives rise to long range electrical transport at low frequencies, while the high frequency dispersion may be correlated to the forward–backward hopping of the ions at high frequencies which requires only a fraction of energy which is involved in the long range diffusion of ions. The hopping frequency (ω_P) is the frequency at which the relaxation effects begin to appear and it was found to shift towards higher frequency side with increase in temperature and can be calculated using Equation 4 and values are given in Table 3.

$$\omega_P = [\sigma_{dc}/A]^{1/n} \tag{4}$$

where ω_P is assumed to be present at σ_{ac} equal to $2\sigma_{dc}$ as depicted in Fig. 10(a) for all glass samples at 323 K temperature. The variation of power law exponent 'n' with temperature for different glass compositions is shown in Fig. 11. It is observed that the value of exponent 'n' ranges from 0.51 to 0.73. Degree of interaction between mobile ions and the host frame work is explained by frequency exponent (n). In the present study, it is found that, value of 'n' increases with temperature, associated with Non-Overlapping Small Polaron Tunnelling Model (NSPT) [42,43]. It is elsewhere reported by Dult et al.; [43] that the smaller value of power exponent parameter signifies the high degree of modification in the network. It is observed from Fig. 11 that, the value of 'n' is the lowest in case of ABP5 sample at all temperatures suggesting high degree of interaction between mobile ions and the frame work.

Due to accumulation of more charges at electrode–electrolyte polarization, a simultaneous sharp decrease in $\sigma^{'}(\omega)$ at lower frequency region is observed. At intermediate frequency regime $(\omega < \omega_p)$, the conductivity is almost frequency independent. This is because the ions travel much faster and can jump from one site to the another unoccupied sites as S. Murugavel et al.; [44] also reported same observation. The dc conductivity is a result of the successful hop of ion to a neighbouring vacant site. When the frequency is higher than that of the hopping frequency $(\omega > \omega_p)$, the ionic conductivity starts increasing with the frequency. The conductivity relaxation phenomena occur when the frequency independent conductivity changes to dispersive conductivity. The observed frequency dependence of conductivity in the present glass systems can be understood on the basis of jump relaxation model [45,46]. According to this model, at lower frequencies, ion can successfully hop to its neighbouring vacant site due to long time periods available at these frequencies contributing to dc conductivity which results into plateau region. Once an ion has completed its "initial hop" from initial site to the neighbouring site, two relaxation processes may be visualized: first, the ion may hop back to its initial position known as correlated forward–backward hopping and second, the surrounding

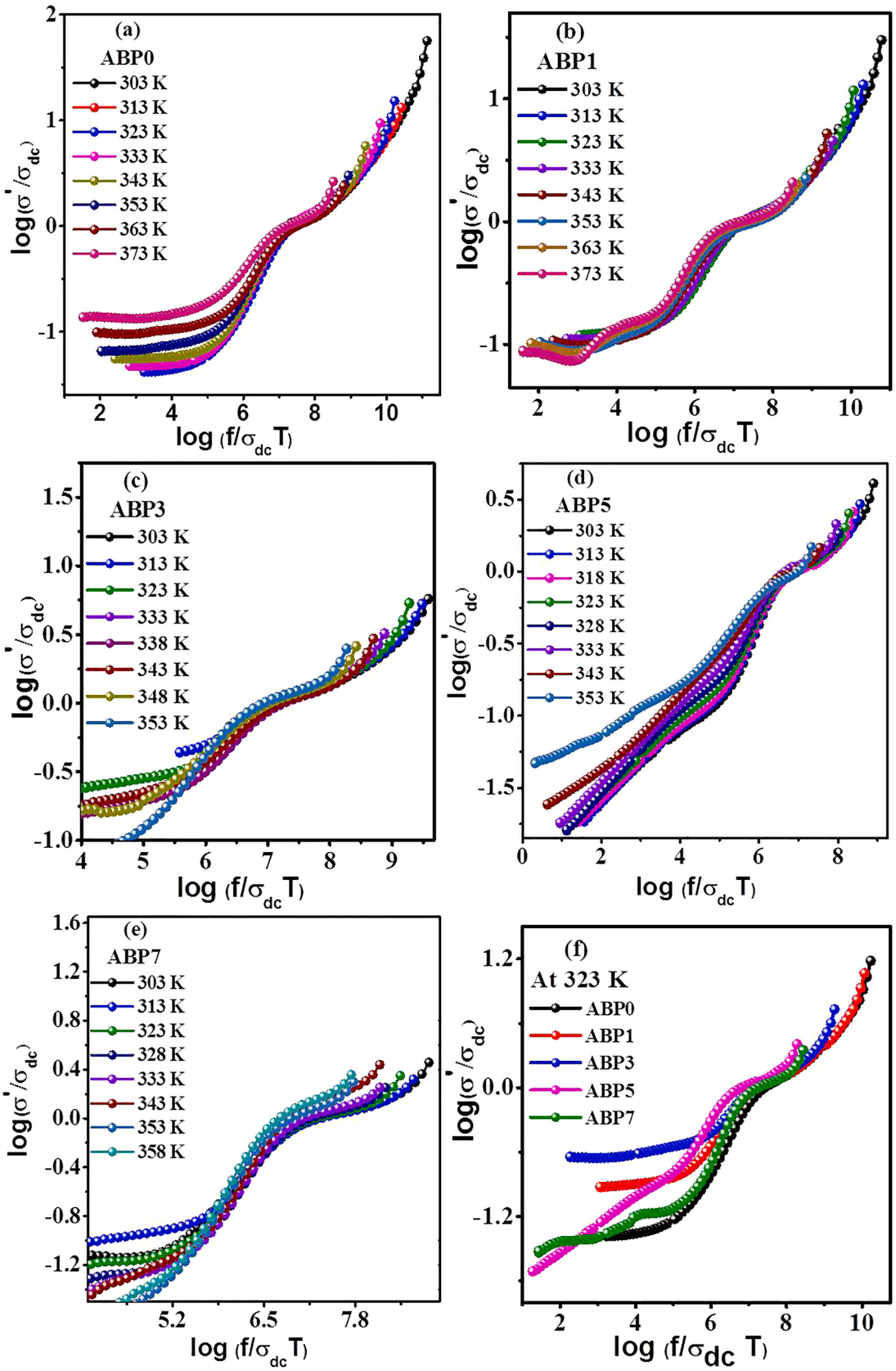

Fig. 13. (a-e) Plots of Scaled conductivity spectra with frequency using Roling formulation at different temperatures and (f) plot of scaled conductivity spectra of all glass samples with frequency at 323 K.

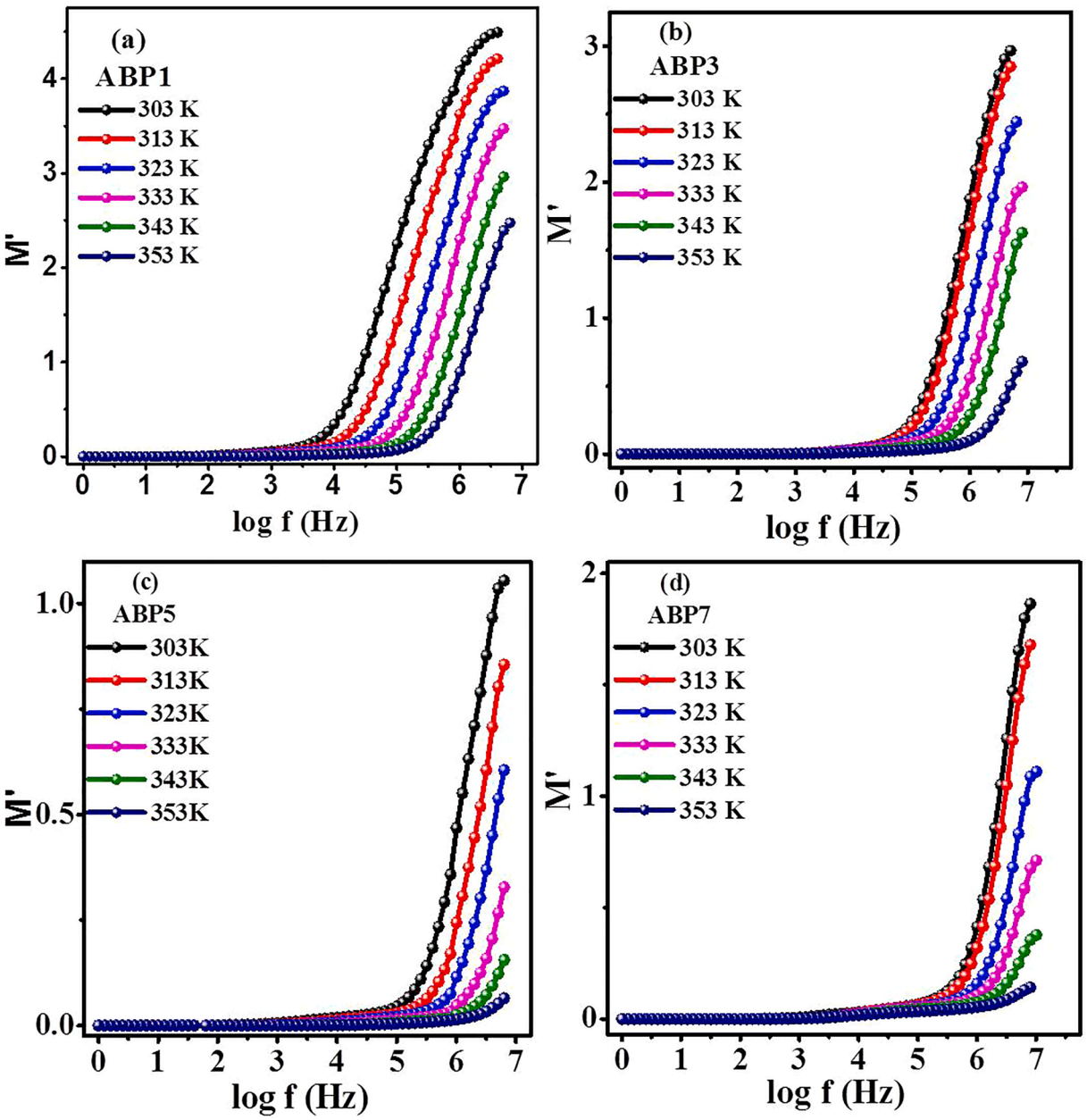

Fig. 14. (a-d) Plots of M' (real part of modulus) vs. logarithmic function of frequency (log f) for ABP1 to ABP7 samples at different temperatures.

(neighbouring) ion cloud will relax with respect to its new position thereby shifting its cage potential. At higher frequencies, the probability for the ion to go back again to its initial site increases due to the short time intervals. This increased probability of correlated forward–backward hopping at higher frequencies along with relaxation of the cage potential leads to the observed high frequency conductivity dispersion in ac conductivity spectra. The mobile ion concentration factor K' [47] is also an important factor in conductivity. It is calculated using Equation 5 and its values are given in Table 3.

$$K' = \frac{\sigma_{dc} T}{\omega_P} \tag{5}$$

The variation of mobile ion concentration factor as a function of temperature in glass samples, is shown in Fig. 12. It is observed that the mobile ion concentration (K') increases slightly upto ABP3 with changing temperature, while a larger increase is observed for ABP5 and ABP7 in the glass samples. The inset of Fig. 12 describes that the charge carrier concentration factor varies almost linearly with increasing AgI up to 5 wt% and then decreases for ABP7 glass sample at room temperature.

Scaling is an important tool to understand the ac conductivity behaviour of ionically conducting glasses. It merges the different data sets to a single master curve, which indicates that the processes can be described by a common physical mechanism on thermodynamic scales or composition [48]. Different methods of scaling approaches have been used by many workers [48-54]. The first ever scaling of σ' spectra was attempted by Summerfield [50] in semiconductors and this approach has been widely utilized by Roling et al.; [48] and its modified version by others [49] for scaling different relaxation spectra of ionically conducting glass systems. In its simplest form, the Summerfield scaling is given as in Equation 6,

$$\frac{\sigma'}{\sigma_{dc}} = F\left(\frac{f}{\sigma_{dc} T}.x\right) \ldots (\text{Summerfield formulation}) \tag{6}$$

where f = frequency, σ_{dc}= conductivity at given temperature, T =

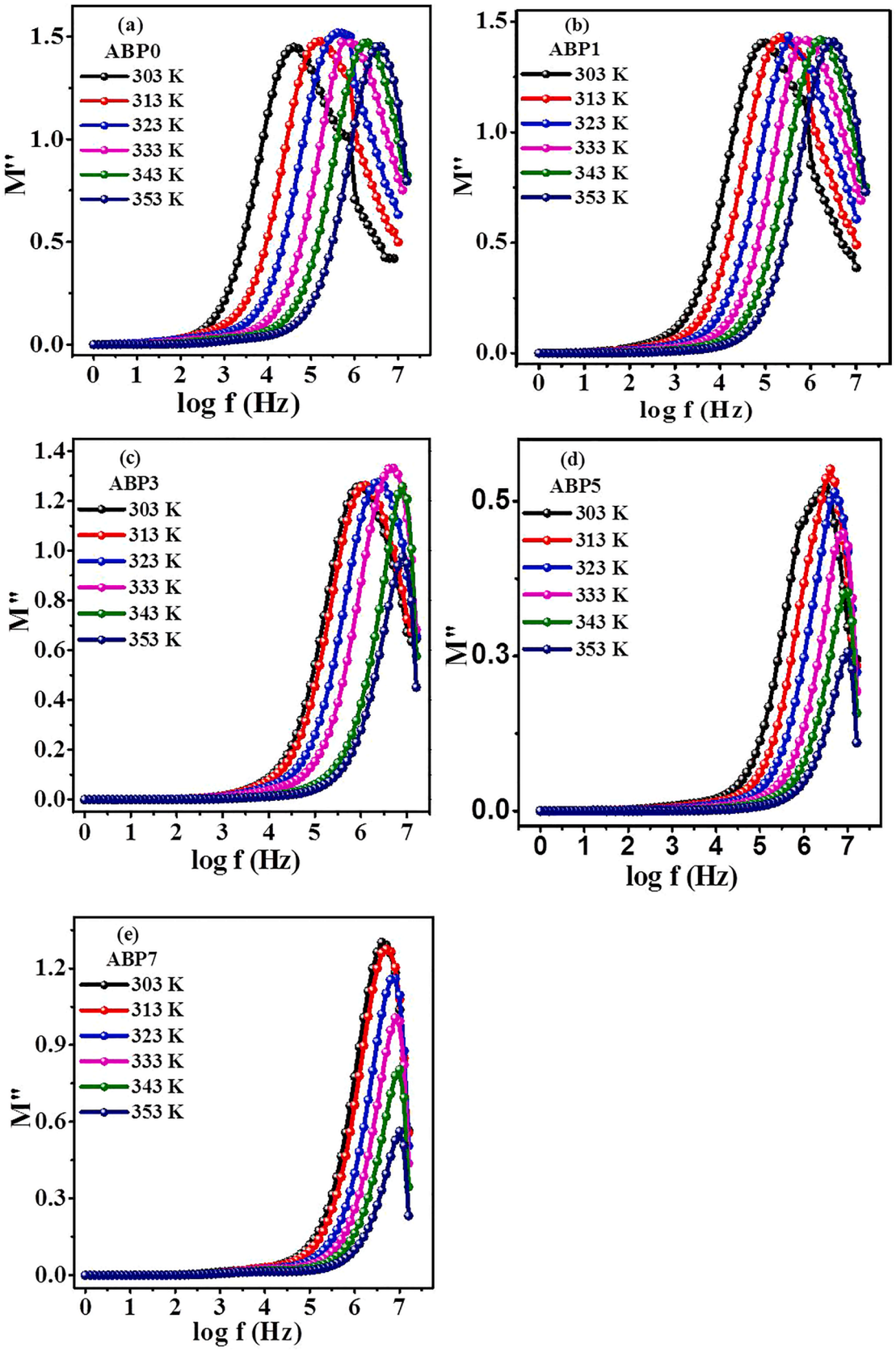

Fig. 15. (a-e) Plots of M‟ (imaginary part) vs. logarithmic function of frequency (log f) for all glass samples at different temperatures.

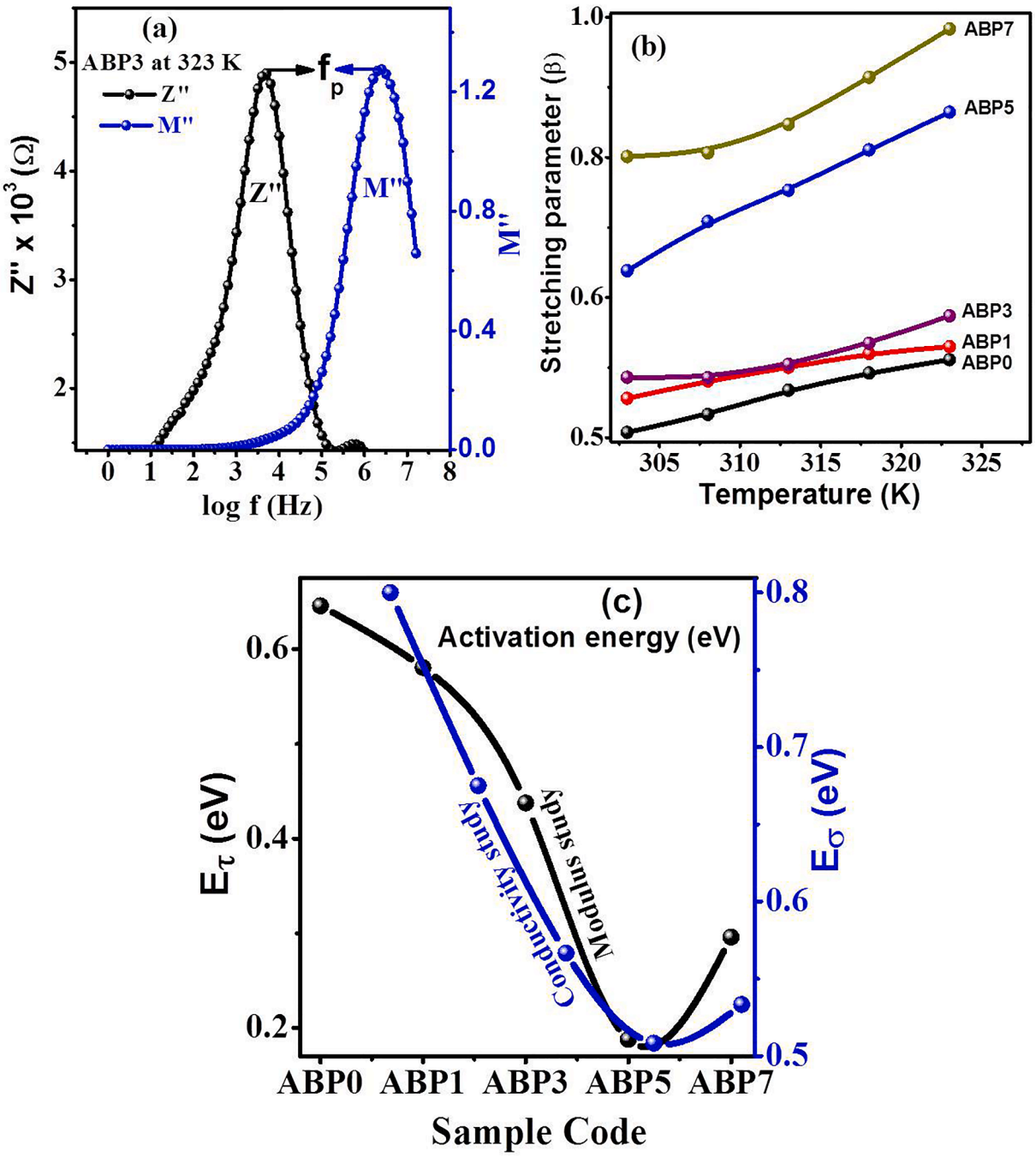

Fig. 16. (a-b) Variation in Z" (imaginary part of impedance) and M" (imginary part of electric modulus) for ABP3 samples at 323 K, (b) Variation of stretching parameter β vs. temperature for all glass samples. (c) Comparison of activation energies E_σ and E_τ obtained from conductivity and modulation relaxation time studies respectively.

absolute temperature, x = concentration factor. If it is assumed that charge carrier concentration remains constant with temperature, the scaling law may be presented in the form of Equation 7,

$$\frac{\sigma'}{\sigma_{dc}} = F\left(\frac{f}{\sigma_{dc}\,T}\right) \ldots(\text{Roling formalism}) \quad (7)$$

Here, ac conductivity data scaled by dc conductivity σ_{dc}, and the frequency axis scaled by different parameters, e.g. $(\sigma_{dc}T)$ or (ω_P), where ω_P is the hopping frequency and T is absolute temperature [49]. In the present study, the Roling's scaling model has been found most appropriate for scaling of the conductivity versus frequency curves [48].

The scaled conductivity spectra for the ABP0 to ABP7 glasses at different temperatures are shown in Fig. 13 (a-e). All conductivity spectra, at different temperatures in Fig. 13, merge near perfectly into a single master curve which indicates the existence of a time temperature superposition (TTS) and a temperature independent conduction mechanism. Fig. 13 (f) shows the scaled conductivity spectra of all the glass compositions at 323 K, which also nearly merge in to a single curve indicating composition independence of ionic conductivity. All the spectra however do not merge at very low frequencies near polarization region. This may be due to change in mobile Ag^+ ion concentration and/or slightly different ion transport behaviour in the glass at a given temperature. According to Dyre et al. [52], TTS is observed in single ion conducting glasses and crystals with structural disorder, because the

disorder of the glass matrix leads to a broad distribution of ion site energies and barrier heights and thus to a broad distribution of jump rates [53,54] and the Coulombic interactions cause a significant spread in the potential energies of the ions.

The scaling approach used here suggests that the conductivity relaxation is a time–temperature and composition independent process in these glasses, in a wide frequency range except at low frequency region, i.e. it depends on the mobile ion concentration [48]. Sidebottom [51] named such scaling as canonical scaling where shape of the ac conductivity spectra is preserved with changing temperature and ion concentration remains invariant.

4.5. Electric modulus study

Frequency independent to frequency dependent conductivity provides the onset of a relaxation phenomenon, which can be discussed in terms of the electrical modulus. In the modulus formalism, the polarization effects are suppressed which are produced due to the electrode–electrolyte interface. Macedo et al.; [55] reported that the Modulus formalism can represent the relaxation processes occurring due to the motion of ions in superionic glasses.

Several models have been discussed by various researchers [48,56-62] to understand ion relaxation and its behaviour as a function of temperature and/ or frequency for ionic conducting systems (glass/ polymer).

According to Macedo et al [55]; the electrical modulus is obtained by reciprocating the complex dielectric permittivity ε^* is as follows

$$M^* = \frac{1}{\varepsilon_0} = M' + iM'' \tag{8}$$

where M' and M'' are the real and imaginary components of electric modulus.

While Moynihan et al.; [62] introduced the Kohlrausch-Williams-Watts (KWW) relaxation function in an empirical manner to represents the width of the M'' peaks which is often associated with a stretching exponent β. They proposed

$$\varnothing(t) = e^{(-t/\tau)^{\beta}} \tag{9}$$

The values of β typically found to be $0 < \beta < 1$ (Non-Debye),which is obtained by fitting the frequency dependent plots of imaginary part of the electric modulus (M'').

Ngai and Kannert [63] have derived the 'coupling model' which shows connection between these two approaches. They have anticipated that the power-law variation of the conductivity is associated with the KWW relaxation mechanism, then Equation (9) can be written as

$$\sigma_{kww} = B\ exp(-E_a/K_BT)\omega^{1-\beta} \tag{10}$$

The activation energy (E_a) related to activation energy for dc conduction (E_σ) and the stretching parameter (β), which is derived from a relaxation process.

$$E_a/E_\sigma = \beta \tag{11}$$

In the present study, the frequency dependent real part of the modulus (M') shows dispersion which reaches to maximum and shifts towards higher frequency depicted in Fig. 14(a-d). A long and flat tail starting from the low frequency up to the intermediate frequency region is observed in the plots of frequency dependent imaginary part of the modulus (M'') curve shown in Fig. 15(a-e). Large capacitance associated with the electrodes is the main reason for such nature. The value of the modulus starts increasing and reaches to a maximum value termed as peak of M'' at higher frequencies which may be due to the bulk effect. It is noted that the M'' peak shifts towards the higher frequency side with temperature, with different peak heights. At all the temperatures, the shapes of M'' curves look alike but differ only by their peak position and FWHM (Full Width at Half Maximum) values as well.

The conductivity relaxation frequency ω_c corresponding to M''_{max} gives the average or characteristic relaxation time by the condition that $\omega_c\tau_c = 1$ [64]. The frequency range below M''_{max} determines the range where charge carriers are mobile over long distances while the frequency range above M''_{max} is the frequency range where the charge carriers are confined to potential wells and are mobile over short ranges only. The continuous shift in the f_{max} position with rise of temperature is attributed to the distribution of frequencies for the barrier cross-over. The width of the M'' curves is interpreted in terms of the distribution of relaxation times which is connected with a distribution of free energy barriers for ionic jumps, in which distribution is increased with increasing disorder or due to the cooperative nature of the conduction process. This temperature dependent behaviour of M'' can be explained on the basis that the charge carriers get thermally activated with an increase in the temperature and hence acquire a rapid movement which leads to a decrease in the relaxation time. Thus, the shifting of the relaxation peak towards higher frequency with temperature suggests the occurrence of temperature dependent relaxation processes in the present glass system. The Ag^+ ions are mobile over long distances in the frequency range below M''_{max} while frequency range above M''_{max} ($f > f_p$), the ions are confined in a narrow dimensional potential-well and free to move over short distances only. The region of the peak therefore is indicative of the transition from long range to short range mobility.

A plot of values of M'' and Z'' with frequency has been shown in Fig. 16(a). It can be seen that there is a mismatch between the peaks of plots of M'' and Z'' versus frequency which confirms the relaxation process in the present glasses due to the localized movement of charge carriers. The obtained M'' data were fitted to the stretched exponential KWW function [62]. The stretching parameter (β), which corresponds to FWHM of M'' curve, is plotted against temperature for all the glass compositions shown in Fig. 16(b). It increases with increase in temperature and composition as well. We note that the frequency exponent 'n' does not obey Ngai's relation $\beta = 1 - n$ [65,66] given in Equation (10). The value of frequency exponent (n) is to be estimated from the high frequency region of the conductivity spectra, while the value of stretching parameter (β) is between the shoulders of the electric modulus peak. The plots of imaginary part of electric modulus are not perfectly fitted in the high frequency regime affects the value of β. The qualitative changes in the values of 'β' and 'n' are in conformity with the fact that both parameters represent the interaction between the ions [65]. The Fig. 9(d) shows the reciprocal temperature dependence of the relaxation time for all the glass compositions and it closely fits to the following Arrhenius relation [67,68]

$$\tau_c = \tau_0 exp[E_\tau/kT] \tag{12}$$

where τ_c is the characteristic relaxation time, τ_0 is the pre-exponential factor and E_τ is the activation energy for τ_c. The activation energy E_σ, obtained from the dc conductivity processes found to be 0.84–0.52 eV, which is the activation energy for long range charge transport and E_τ from the relaxation processes, which corresponds to the short distance transport found to be 0.64–0.29 eV, are appear to be different as depicted in the Fig. 16(c). It suggests that the dc conduction process and the conductivity relaxation processes, both are activated by slightly different mechanisms [67,68].

To understand dielectric mechanism, scaling of modulus spectra have been suggested by various workers [65,69-75]. The Ac universality was first recognized by Taylor (1956–59), shown dielectric loss for different ionic glass composition fell on a single plot against scaled frequency. Later, Isard (1961) [76] relabelled Taylor's axis by plotting dielectric loss against logarithmic function of product of frequency (f) and dc resistivity (σ_{dc}) known as Taylor-Isard formulation. The constant (C) is proportional to the inverse of temperature.

$$\sigma = \frac{\sigma(\omega)}{\sigma_0} = \mathrm{F}\left(\mathrm{c}\frac{\omega}{\sigma_0}\right) \ldots (\text{Taylor} - \text{Isard formulation}) \tag{13}$$

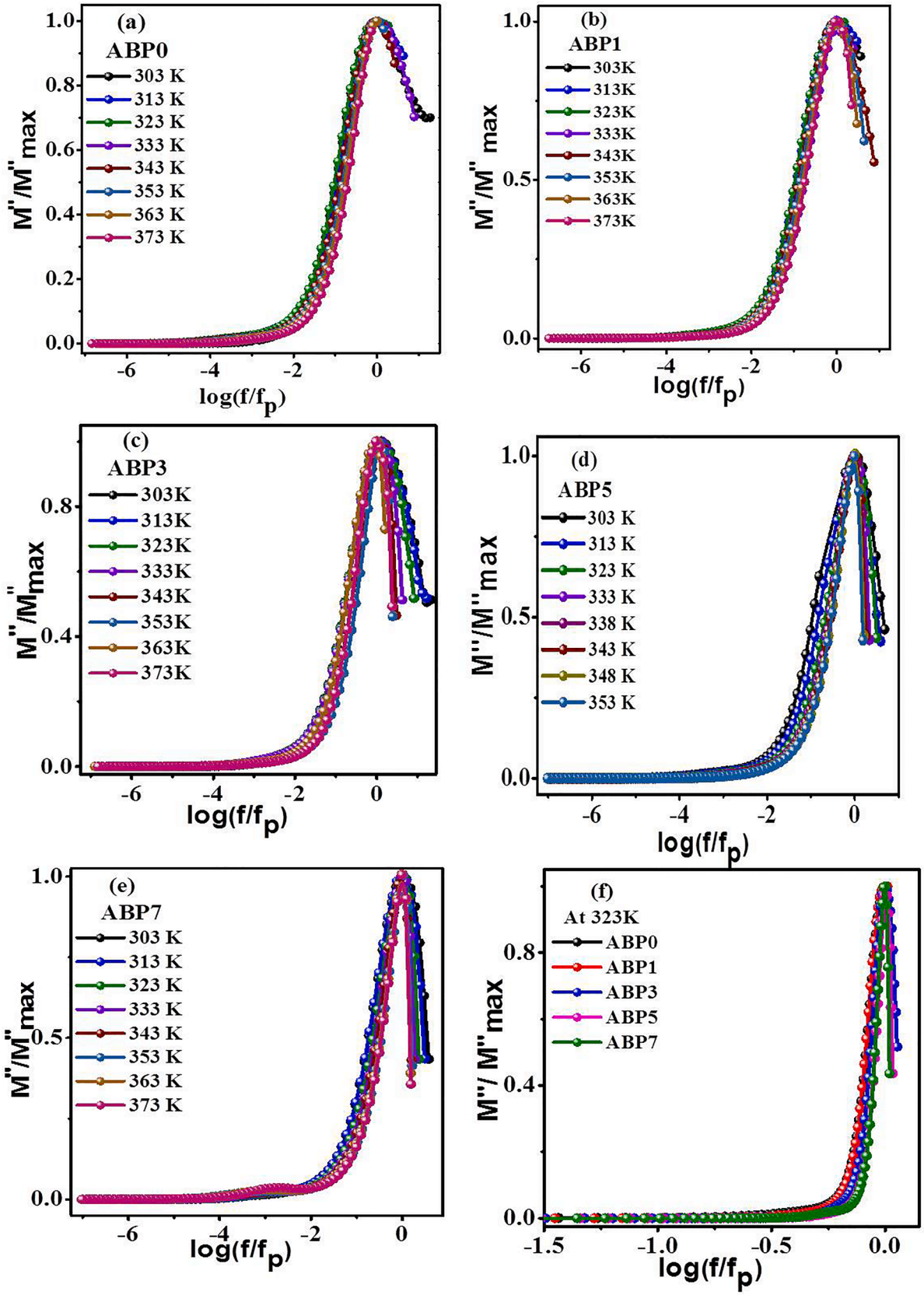

Fig. 17. (a-e) Scaled modulus spectra ($M^{''}/M^{''}_{max}$) plotted against normalized frequency (f/f_P) at different temperatures, (f) Scaled modulus spectra ($M^{''}/M^{''}_{max}$) plotted against normalized frequency (f/f_P) for all glass samples at 323 K.

Based on AC universality (disorder solids), it is always possible to scale measurements of the frequency dependent parameter at a different temperature/ for various glass compositions into a single master curve by various workers [40,48,56,77-81].

The normalized value of imaginary part of modulus scaled with the frequency, dc conductivity, temperature and carrier concentration was initially suggested by Summerfield and it is modified by Roling [74],

$$\frac{M''}{M''_p} = F\left(\frac{f}{\sigma_{dc} T}\right) \ldots(\text{Roling model formalism}) \quad (14)$$

The empirical formula for modulus scaling was suggested by Ghosh [66], where both the axis are normalized with its peak values.

$$\frac{M''}{M''_p} = F\left(\frac{f}{f_p}\right) \ldots(\text{Ghosh model formalism}) \quad (15)$$

To warrant a better insight of the relaxation processes for ion conducting materials like glasses and polymer systems, we have tried to attempt the scaling of imaginary component of modulus (M'') with frequency and temperature using all probable alternative functions. However, Roling and Ghosh Models had nearly successfully scaled the Modulus values. Hence, we have chosen the horizontal axis scaled with the normalized frequency (f/f_p) and for imaginary part of modulus at different temperatures scaled with normalized Modulus (M''/M''_{max}) shown in Fig. 17 (a to e) which exhibit the scaling of the M'' curves by Ghosh Model ($M''/M''_{max} \rightarrow log(f/f_{max})$, for all the compositions at different temperatures. The data for different temperatures are found to merge near perfectly into a single master curve, which suggests that all the dynamic processes occurring at different time scales exhibit the same activation energy and the distribution of relaxation times is independent of temperature or the ionic relaxation mechanism is temperature independent or a Time Temperature Superposition (TTS) holds. It can be seen from Fig. 17(f) that the scaling of M'' curve at any particular temperature for all the samples also results into a single master curve, which implies that the conductivity relaxation is also independent of the composition of the glass. Thus, it is attributed that the relaxation process in the $[Ag_2O: (B_2O_3\text{-}P_2O_5)]$ glass system mixed with AgI do not depend on temperature as well as composition.

5. Conclusion

In the present glassy electrolyte x. AgI: (100-x).$[Ag_2O: (B_2O_3\text{-}P_2O_5)]$ prepared by a rapid melt quench method, the ionic conductivity considerably increases with the addition of AgI up to 5 wt% giving a maximum ionic conductivity $6.24x10^{-5}$ S/cm at room temperature. The present borophosphate glass system follows the silver ion conduction mechanism according to Anderson-Stuart (A-S) model. The electric modulus study confirms the distributed relaxation time and non-Debye nature of glassy electrolytes as well. The values of stretching parameter 'β' indicate the deviation from the ideal Debye nature. The scaling of conductivity and electric modulus confirmed that all the dynamic processes occurring at different time scales exhibit the slightly different activation energy and the distribution of relaxation times is independent of temperature as well as the composition of the glass. Such glasses may be a good candidate for solid state batteries or as a supercapacitor.

Declaration of Competing Interest

The authors declare that they have no known competing financial interests or personal relationships that could have appeared to influence the work reported in this paper.

Acknowledgements

Authors also would like to express the acknowledgement to Dr. N. Jamnapara for providing XRD facility at FCIPT-Gandhinagar and to Dr. M. Patel for the TG-DTA facility at GIRDA-Vadodara.

Funding

This research did not receive any specific grant from funding agencies in the public, commercial or not for profit sectors.

Data availability

The raw data required to reproduce these findings are available to download from [INSERT PERMANENT WEB LINK(s)]. The processed data required to reproduce these findings are available to download from [INSERT PERMANENT WEB LINK(s)].

Appendix A. Supplementary data

Supplementary data to this article can be found online at https://doi.org/10.1016/j.mseb.2020.114857.

References

[1] D. Kunze, in "Fast Ion Transport in Solids," edited by W. van Gool (North-Holland Publ., Amsterdam, 1973) p. 405.
[2] R.C. Agrawal, R.K. Gupta, Superionic solids: composite electrolyte phase – an overview, J. Mater. Sci. 34 (6) (1999) 1131–1162, https://doi.org/10.1023/A:1004598902146.
[3] H.L. Tuller, D.P. Button, D.R. Uhlmann, Fast ion transport in oxide glasses, J. Non-Cryst. Solids 40 (1–3) (1980) 93–118, https://doi.org/10.1016/0022-3093(80)90096-4.
[4] J.L. Souquet, Electrochemical properties of ionically conductive glasses, Solid State Ionics 5 (C) (1981) 77–82, https://doi.org/10.1016/0167-2738(81)90198-3.
[5] J.B. Goodenough, Fast ionic conduction in solids, Proc. R. Soc. Lond. A 393 (1805) (1984) 215–234.
[6] Chandra, S., 1984. Fast proton transport in solids. In Materials Science Forum (Vol. 1, pp. 153–169). Trans Tech Publications Ltd. doi: 10.4028/www.scientific.net/MSF.1.153.
[7] C.E. Kim, H.C. Hwang, M.Y. Yoon, B.H. Choi, H.J. Hwang, Fabrication of a high lithium ion conducting lithium borosilicate glass, J. Non-Cryst. Solids 357 (15) (2011) 2863–2867, https://doi.org/10.1016/j.jnoncrysol.2011.03.022.
[8] A. Pradel, M. Ribes, Ionic conductivity of chalcogenide glasses, in: Chalcogenide Glasses, Elsevier Ltd., 2013, pp. 169–208, https://doi.org/10.1533/9780857093561.1.169.
[9] N.J. Kim, S.H. Im, D.H. Kim, D.K. Yoon, B.K. Ryu, Structure and properties of borophosphate glasses, Electron. Mater. Lett. 6 (3) (2010) 103–106, https://doi.org/10.3365/eml.2010.09.103.
[10] M.P.F. Graça, H. Fawzy, Y. Badr, M.M. Elokr, C. Nico, R. Soares, M.A. Valente, Electrical, dielectric and structural properties of borovanadate glass systems doped with samarium oxide, Physica Status Solidi (C) Current Topics in Solid State Physics 8 (11–12) (2011) 3107–3110, https://doi.org/10.1002/pssc.201000762.
[11] B. Deb, S. Kabi, A. Ghosh, Mixed glass former effect in silver molybdophosphate and borophosphate glasses, AIP Conference Proceedings 1349 (2011) 519–520, https://doi.org/10.1063/1.3605961.
[12] L. Koudelka, P. Mošner, J. Šubčík, Study of structure and properties of modified borophosphate glasses. In IOP Conference Series: Materials Science and Engineering (Vol. 2), 2009. doi: 10.1088/1757-899X/2/1/012015.
[13] K. Funke, R.D. Banhatti, P. Grabowski, J. Nowinski, W. Wrobel, R. Dinnebier, O. Magdysyuk, Low-temperature α-AgI confined in glass: structure and dynamics, Solid State Ionics 271 (2015) 2–9, https://doi.org/10.1016/j.ssi.2014.09.033.
[14] R. Suresh Kumar, K. Hariharan, AC conductivity and electrical relaxation studies on 10CuI-60AgI-30V2O5 glasses, Mater. Chem. Phys. 60 (1) (1999) 28–38, https://doi.org/10.1016/S0254-0584(99)00057-7.
[15] H. Iwahara, Conducting Materials: Solid-ionic and Super-ionic. In Encyclopaedia of Materials: Science and Technology (pp. 1482–1496). Elsevier, 2001. doi: 10.1016/b0-08-043152-6/00269-2.
[16] V.K. Deshpande, Science and technology of glassy solid electrolytes. In IOP Conference Series: Materials Science and Engineering (Vol. 2), 2009. doi: 10.1088/1757-899X/2/1/012011.
[17] S. Hoshino, Structure and dynamics of solid state ionics, Solid State Ionics 48 (3–4) (1991) 179–201, https://doi.org/10.1016/0167-2738(91)90032-7.
[18] T. Minami, Y. Ikeda, M. Tanaka, Infrared spectra, glass transition temperature, and conductivity of superionic conducting glasses in the systems $AgXAg_2OB_2O_3$ (X = I, Br), J. Non-Cryst. Solids 52 (1–3) (1982) 159–169, https://doi.org/10.1016/0022-3093(82)90290-3.
[19] Aldo Magistris, Gaetano Chiodelli, Michel Duclot, Silver borophosphate glasses : Ion transport, thermal stability and electrochemical behaviour, Solid State Ionics, Volumes 9–10, Part 1,1983,Pages 611-615,ISSN 0167-2738, doi: 10.1016/0167-2738(83)90303-X.

[20] P. Sharma, D.K. Kanchan, M. Pant, M.S. Jayswal, N. Gondaliya, Effect of AgI on conduction mechanism in silver-vanadate superionic glasses, New J. Glass Ceramics 01 (03) (2011) 112–118, https://doi.org/10.4236/njgc.2011.13016.
[21] G. Kaur, O.P. Pandey, K. Singh, D. Homa, B. Scott, G. Pickrell, A review of bioactive glasses: their structure, properties, fabrication and apatite formation, J. Biomed. Mater. Res. A 102 (1) (2014) 254–274, https://doi.org/10.1002/jbm.a.34690.
[22] K.J. Hamam, G. Mezei, Z. Khattari, et al., Temperature and frequency effect on the electrical properties of bulk nickel phthalocyanine octacarboxylic acid (Ni-Pc (COOH)8), Appl. Phys. A 125 (2019) 7, https://doi.org/10.1007/s00339-018-2147-7.
[23] K.J. Hamam, F. Salman, Dielectric constant and electrical study of solid-state electrolyte lithium phosphate glasses, Appl. Phys. A 125 (2019) 621, https://doi.org/10.1007/s00339-019-2868-2.
[24] C. Angell, Mobile ions in amorphous solids, Annu. Rev. Phys. Chem. 43 (1) (1992) 693–717, https://doi.org/10.1146/annurev.physchem.43.1.693.
[25] J.E. Shelby, CHAP: Structures of glasses, Introduction to Glass Science and Technology (2), The Royal Society of Chemistry 72–110 (2005), https://doi.org/10.1039/9781847551160-00072.
[26] V.N. Rai, B.N. Raja Sekhar, D.M. Phase, S.K. Deb, 2014. Effect of gamma irradiation on the structure and valence state of Nd in phosphate glass. cond-mat.mtrl-sci., 1-30. https://arxiv.org/abs/1406.4686.
[27] Y.M. Lai, X.F. Liang, S.Y. Yang, J.X. Wang, L.H. Cao, B. Dai, Raman and FTIR spectra of iron phosphate glasses containing cerium, J. Mol. Struct. 992 (1–3) (2011) 84–88, https://doi.org/10.1016/j.molstruc.2011.02.049.
[28] J.J. Hudgens, S.W. Martin, Mid-IR and far-IR investigation of AgI-doped silver diborate glasses, Phys. Rev. B – Condensed Matter Mater. Phys. 53 (9) (1996) 5348–5355, https://doi.org/10.1103/PhysRevB.53.5348.
[29] M. Htut, M. Lwin, P. Kaung, S. Htoon, Infrared Spectroscopic Study on the Structure of Ag 2 O.B 2 O 3 Glasses @BULLET. Jour. Myam Acad. Arts & Sc, IV(2), 2006. Retrieved from http://www.iaea.org/inis/collection/NCLCollectionStore/_Public/40/057/40057374.pdf.
[30] H.A. Othman, H.S. Elkholy, I.Z. Hager, FTIR of binary lead borate glass: Structural investigation, J. Mol. Struct. 1106 (2016) 286–290, https://doi.org/10.1016/j.molstruc.2015.10.076.
[31] A.M. Efimov, IR fundamental spectra and structure of pyrophosphate glasses along the 2ZnO • P2O5-2Me2O • P2O5 join (Me being Na and Li), J. Non-Cryst. Solids 209 (3) (1997) 209–226, https://doi.org/10.1016/S0022-3093(96)00562-5.
[32] C. Gautam, A.K. Yadav, A.K. Singh, A review on infrared spectroscopy of borate glasses with effects of different additives, ISRN Ceramics 2012 (2012) 1–17, https://doi.org/10.5402/2012/428497.
[33] L. Balachander, G. Ramadevudu, M. Shareefuddin, R. Sayanna, Y.C. Venudharc, IR analysis of borate glasses containing three alkali oxides, Science Asia 39 (3) (2013) 278–283, https://doi.org/10.2306/scienceasia1513-1874.2013.39.278.
[34] S. Kabi, A. Ghosh, Mixed glass former effect in AgI doped silver borophosphate glasses, Solid State Ionics 262 (2014) 778–781, https://doi.org/10.1016/j.ssi.2013.09.028.
[35] P.N. Rao, E. Ramesh Kumar, B. Appa Rao, Structural, electrical, and transport number studies of AgI-doped silver borotellurite fast ion conducting glass system, Ionics 24 (12) (2018) 3885–3895, https://doi.org/10.1007/s11581-018-2550-2.
[36] K. Srinivas, P. Sarah, S.V. Suryanarayana, Impedance spectroscopy study of polycrystalline Bi6Fe2Ti3O18, Bull. Mater. Sci. 26 (2) (2003) 247–253, https://doi.org/10.1007/BF02707799.
[37] A. Pan, A. Ghosh, Activation energy and conductivity relaxation of sodium tellurite glasses, Phys. Rev. B – Condensed Matter Mater. Phys. 59 (2) (1999) 899–904, https://doi.org/10.1103/PhysRevB.59.899.
[38] W. Wang, R. Christensen, B. Curtis, S.W. Martin, J. Kieffer, A new model linking elastic properties and ionic conductivity of mixed network former glasses, Phys. Chem. Chem. Phys. 20 (3) (2018) 1629–1641, https://doi.org/10.1039/c7cp04534d.
[39] M.L.F. Nascimento, E. Do Nascimento, S. Watanabe, Test of anderson-stuart model and the "Universal" conductivity in rubidium and cesium silicate glasses, Braz. J. Phys. 35 (3 A) (2005) 626–631, https://doi.org/10.1590/S0103-97332005000400007.
[40] Dynamic processes in ionic glasses, C. Austin Angell, Chem. Rev., 1990 90 (3), 523-542, doi: 10.1021/cr00101a006.
[41] S.H. Chung, K.R. Jeffrey, J.R. Stevens, L. Börjesson, Dynamics of silver ions in (AgI) x-(Ag2O-nB2O3)1–x glasses: a Ag109 nuclear magnetic resonance study, Phys. Rev. B 41 (10) (1990) 6154–6164, https://doi.org/10.1103/PhysRevB.41.6154.
[42] N. Chakchouk, B. Louati, K. Guidara, Electrical properties and conduction mechanism study by OLPT model of NaZnPO4 compound, Mater. Res. Bull. 99 (2018) 52–60, https://doi.org/10.1016/j.materresbull.2017.10.046.
[43] M. Dult, R.S. Kundu, S. Murugavel, R. Punia, N. Kishore, Conduction mechanism in bismuth silicate glasses containing titanium, Physica B 452 (2014) 102–107, https://doi.org/10.1016/j.physb.2014.07.004.
[44] S. Murugavel, M. Upadhyay, A.C. conduction in amorphous semiconductors, J. Indian Inst. Sci. (2011).
[45] K. Funke, Debye-Hückel-type relaxation processes in solid ionic conductors, Z. Phys. Chem. 154 (Part_1_2) (1987) 251–295, https://doi.org/10.1524/zpch.1987.154.Part_1_2.251.
[46] K. Funke, Jump relaxation in solid ionic conductors, Solid State Ionics 28–30 (PART 1) (1988) 100–107, https://doi.org/10.1016/S0167-2738(88)80015-8.
[47] D.P. Almond, A.R. West, Comments on the analyses of AC conductivity data for single crystal Na β-alumina at low temperatures, J. Electroanal. Chem. 193 (1–2) (1985) 49–55, https://doi.org/10.1016/0022-0728(85)85051-8.
[48] B. Roling, A. Happe, K. Funke, M.D. Ingram, Carrier concentrations and relaxation spectroscopy: new information from scaling properties of conductivity spectra in ionically conducting glasses, Phys. Rev. Lett. 78 (11) (1997) 2160–2163, https://doi.org/10.1103/PhysRevLett.78.2160.
[49] A. Ghosh, A. Pan, Scaling of the conductivity spectra in ionic glasses: Dependence on the structure, Phys. Rev. Lett. 84 (10) (2000) 2188–2190, https://doi.org/10.1103/PhysRevLett.84.2188.
[50] S. Summerfield, Universal low-frequency behaviour in the a.c. hopping conductivity of disordered systems. Philosophical Magazine B: Physics of Condensed Matter; Statistical Mechanics, Electronic, Optical and Magnetic Properties, 52(1), 9–22, 1985. doi: 10.1080/13642818508243162.
[51] D.L. Sidebottom, Colloquium: Understanding ion motion in disordered solids from impedance spectroscopy scaling, Rev. Mod. Phys. 81 (3) (2009) 999–1014, https://doi.org/10.1103/RevModPhys.81.999.
[52] J.C. Dyre, P. Maass, B. Roling, D.L. Sidebottom, Fundamental questions relating to ion conduction in disordered solids, Rep. Prog. Phys. 72 (4) (2009), https://doi.org/10.1088/0034-4885/72/4/046501.
[53] I. Svare, Conductivity and NMR relaxation from ionic motion in disordered glasses with distributions of barriers, Solid State Ionics 125 (1) (1999) 47–53, https://doi.org/10.1016/S0167-2738(99)00157-5.
[54] M. Vogel, C. Brinkmann, H. Eckert, A. Heuer, Origin of nonexponential relaxation in a crystalline ionic conductor: a multidimensional 109Ag NMR study, Phys. Rev. B – Condensed Matter Mater. Phys. 69 (9) (2004), https://doi.org/10.1103/PhysRevB.69.094302.
[55] P.B. Macedo, C.T. Moynihan, R. Bose, The role of ionic diffusion in polarization in vitreous ionic conductors, Phys. Chem. Glasses 13 (1972) 171–179.
[56] J.C. Dyre, T.B. Schrøder, Universality of ac conduction in disordered solids, Rev. Mod. Phys. 72 (3) (2000) 873–892, https://doi.org/10.1103/RevModPhys.72.873.
[57] D.L. Sidebottom, J. Zhang, Scaling of the ac permittivity in ion-conducting glasses, Phys. Rev. B – Condensed Matter Mater. Phys. 62 (9) (2000) 5503–5507, https://doi.org/10.1103/PhysRevB.62.5503.
[58] H.K. Patel, S.W. Martin, Fast ionic conduction in Na2SB2S3 glasses: Compositional contributions to nonexponentiality in conductivity relaxation in the extreme low-alkali-metal limit, Phys. Rev. B 45 (18) (1992) 10292–10300, https://doi.org/10.1103/PhysRevB.45.10292.
[59] D. Sidebottom, P. Green, R. Brow, Scaling parallels in the non-Debye dielectric relaxation of ionic glasses and dipolar supercooled liquids, Phys. Rev. B – Condensed Matter Mater. Phys. 56 (1) (1997) 170–177, https://doi.org/10.1103/PhysRevB.56.170.
[60] Patel, Hitendra Kumar, Impedance spectroscopy and NMR studies of fast ion conducting chalcogenide glasses (1993). Retrospective Theses and Dissertations. 10850. https://lib.dr.iastate.edu/rtd/10850.
[61] D.L. Sidebottom, P.F. Green, R.K. Brow, Comparison of KWW and power law analyses of an ion-conducting glass, J. Non-Cryst. Solids 183 (1–2) (1995) 151–160, https://doi.org/10.1016/0022-3093(94)00587-7.
[62] C.T. Moynihan, Analysis of electrical relaxation in glasses and melts with large concentrations of mobile ions, J. Non-Cryst. Solids 172–174 (PART 2) (1994) 1395–1407, https://doi.org/10.1016/0022-3093(94)90668-8.
[63] K.L. Ngai, O. Kanert, Comparisons between the coupling model predictions, Monte Carlo simulations and some recent experimental data of conductivity relaxations in glassy ionics, Solid State Ionics 53–56 (PART 2) (1992) 936–946, https://doi.org/10.1016/0167-2738(92)90275-T.
[64] M.S. Jayswal, D.K. Kanchan, P. Sharma, N. Gondaliya, Relaxation process in PbI2-Ag2O-V2O 5–B2O3 system: Dielectric, AC conductivity and modulus studies, Materials Science and Engineering B: Solid-State Materials for Advanced Technology 178 (11) (2013) 775–784, https://doi.org/10.1016/j.mseb.2013.03.013.
[65] K.L. Ngai, G.N. Greaves, C.T. Moynihan, Correlation between the activation energies for ionic conductivity for short and long time scales and the kohlrausch stretching parameter β for ionically conducting solids and melts, Phys. Rev. Lett. 80 (5) (1998) 1018–1021, https://doi.org/10.1103/PhysRevLett.80.1018.
[66] A. Pan, A. Ghosh, Relaxation dynamics of lithium ions in lead bismuthate glasses, Phys. Rev. B – Condensed Matter Mater. Phys. 62 (5) (2000) 3190–3195, https://doi.org/10.1103/PhysRevB.62.3190.
[67] S Bhattacharya, A Ghosh,Conductivity relaxation in some fast ion-conducting AgI–Ag2O–V2O5 glasses, Solid State Ionics, 161(1–2), 2003, 61–65, ISSN 0167-2738, doi: 10.1016/S0167-2738(03)00277-7.
[68] A. Dutta, A. Ghosh, Ionic conductivity of Li2O–BaO–Bi2O3 glasses, J. Non-Crystalline Solids, 351(3), 2005, 203-208, ISSN 0022-3093, doi: 10.1016/j.jnoncrysol.2004.11.010.
[69] K. Ngai, R. Rendell, Interpreting the real part of the dielectric permittivity contributed by mobile ions in ionically conducting materials, Phys. Rev. B – Condensed Matter Mater. Phys. 61 (14) (2000) 9393–9398, https://doi.org/10.1103/PhysRevB.61.9393.
[70] D.D. Ramteke, R.S. Gedam, Study of Li2O-B2O3-Dy2O 3 glasses by impedance spectroscopy, Solid State Ionics 258 (2014) 82–87, https://doi.org/10.1016/j.ssi.2014.02.006.
[71] M.D. Ingram, Ionic conductivity and glass structure, Philosophical Magazine B: Physics of Condensed Matter; Statistical Mechanics, Electronic, Optical and Magnetic Properties 60 (6) (1989) 729–740, https://doi.org/10.1080/13642818908209739.
[72] A.S. Nowick, B.S. Lim, Analysis of ac conductivity data for Na2O•3SiO2 glass by stretched exponential and Jonscher power-law methods, J. Non-Cryst. Solids 172–174 (PART 2) (1994) 1389–1394, https://doi.org/10.1016/0022-3093(94)90667-X.
[73] J.M. Bobe, J.M. Réau, J. Senegas, M. Poulain, F- ion conductivity and diffusion properties in ZrF4-based fluoride glasses with various NaF concentrations (0 ≤

xNaF ≤ 0.45), Solid State Ionics 82 (1–2) (1995) 39–52, https://doi.org/10.1016/0167-2738(95)00192-9.
[74] B. Roling, What do electrical conductivity and electrical modulus spectra tell us about the mechanisms of ion transport processes in melts, glasses, and crystals? J. Non-Cryst. Solids 244 (1) (1999) 34–43, https://doi.org/10.1016/S0022-3093(98)00847-3.
[75] N.H. Vasoya, P.K. Jha, K.G. Saija, S.N. Dolia, K.B. Zankat, K.B. Modi, Electric modulus, scaling and modeling of dielectric properties for Mn2+-Si4+ co-substituted Mn-Zn Ferrites, J. Electron. Mater. 45 (2) (2016) 917–927, https://doi.org/10.1007/s11664-015-4224-4.
[76] J.O. Isard, Proc. Inst. Electr. Eng. 109B, 440–447 (1961). A study of the migration loss in glass and a generalized method of calculating the rise of dielectric loss with temperature, Suppl. No. 22, [The Institution of Electrical Engineers, Paper No. 3636].
[77] A.E. Owen, 1963, Electric conduction and dielectric relaxation in glass, in Progress in Ceramic Science, Vol. 3, edited by J. E. Burke (Macmillan, New York), pp. 77–196.
[78] M. Tomozawa, Dielectric characteristics of glass, in Treatise on Materials Science, Vol. 12, edited by M. Tomozawa (Academic, New York), pp. 283–345, 1977.
[79] H. Kahnt, 'Ionic transport in oxide glasses and frequency dependence of conductivity', Ber. Bunsenges. Phys. Chem. 95 (1991) 1021–1025.
[80] A. Ghosh, M. Sural, A new scaling property of fluoride glasses: concentration and temperature independence of the conductivity spectra, Europhys. Lett. 47 (1999) 688–693.
[81] J.O. Isard, Dielectric dispersion in amorphous conductors, J. Non-Cryst. Solids 4 (1970) 357–365.